Proton and Ion Linear Accelerators

Week 2, part 1

Yuri Batygin and Sergey Kurennoy
LANL

June 24, 2019

Los Alamos NATIONAL LABORATORY EST. 1943

NNSA National Nuclear Security Administration

Operated by Los Alamos National Security, LLC for the U.S. Department of Energy's NNSA

LA-UR-17-24573

Proton and Ion Linear Accelerators – Week 2, Part 1

- **Why linacs & RF together?**
- **Reminder: basics of linacs**
- **RF cavities**
- **Accelerating structures: RFQ, DTL, CCL, etc.**
- **Electromagnetic (EM) design of accelerating structures. Tools.**
- **Linac components**

Sources:

T.P. Wangler. *RF linear accelerators*, Wiley-VCH, 2nd Ed., 2008.

Handbook of Accelerator Physics and Engineering. Eds. A. Chao *et al*. World Scientific, 2013.

Why linacs & RF together?

Linear accelerator (linac) - **a device that accelerates charged particles in a straight line.**

Linac types:

- **electrostatic – e.g., old TV or CRT monitor**
- **induction – electric field is produced by changing magnetic flux**
- **Radio-Frequency (RF).**

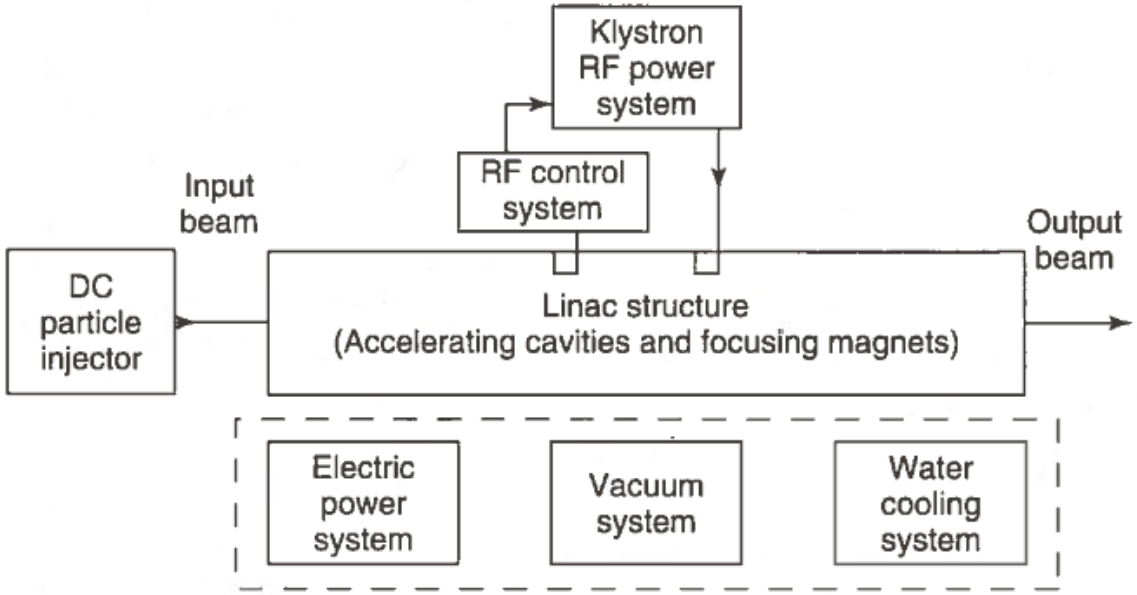

Why linacs & RF together?

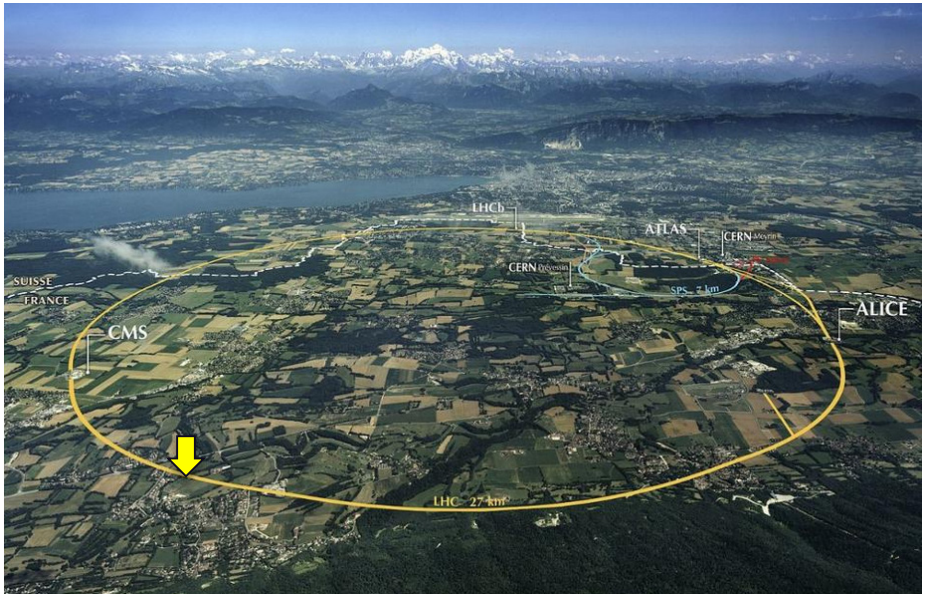

LHC – circular p-p collider (2008): 27 km, but RF acceleration section <100 m. 8 SC 400.8-MHz RF cavities per ring; 8-16 MV; each cavity is only ~2 m long and powered by one klystron (16 klystrons total).

LHC RF section = 2 short linacs!

SLAC – electron linac (1968): 3 km, and RF acceleration "section" ~3 km. 240 2856-MHz klystrons (design - 960), each with 50-MW peak power (x2 with pulse compression), provide total voltage up to ~50 GV (SLC, 1989).

Why linacs & RF together?

SLAC klystron gallery

SLAC linac (30’ below)

960 traveling-wave structures (x3m)

LHC 4 RF cavities in cryo-module

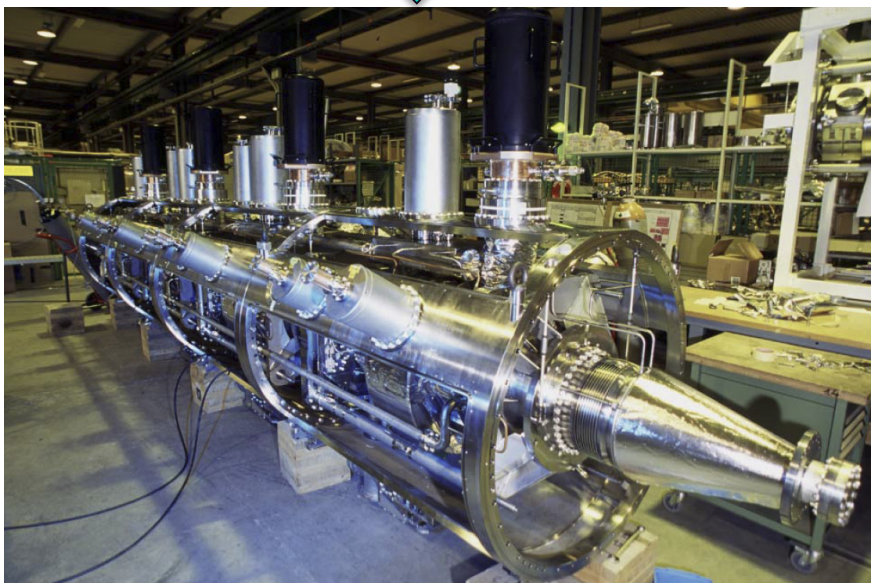

Why linacs & RF together?

LANSCE (LAMPF) linac (1972)

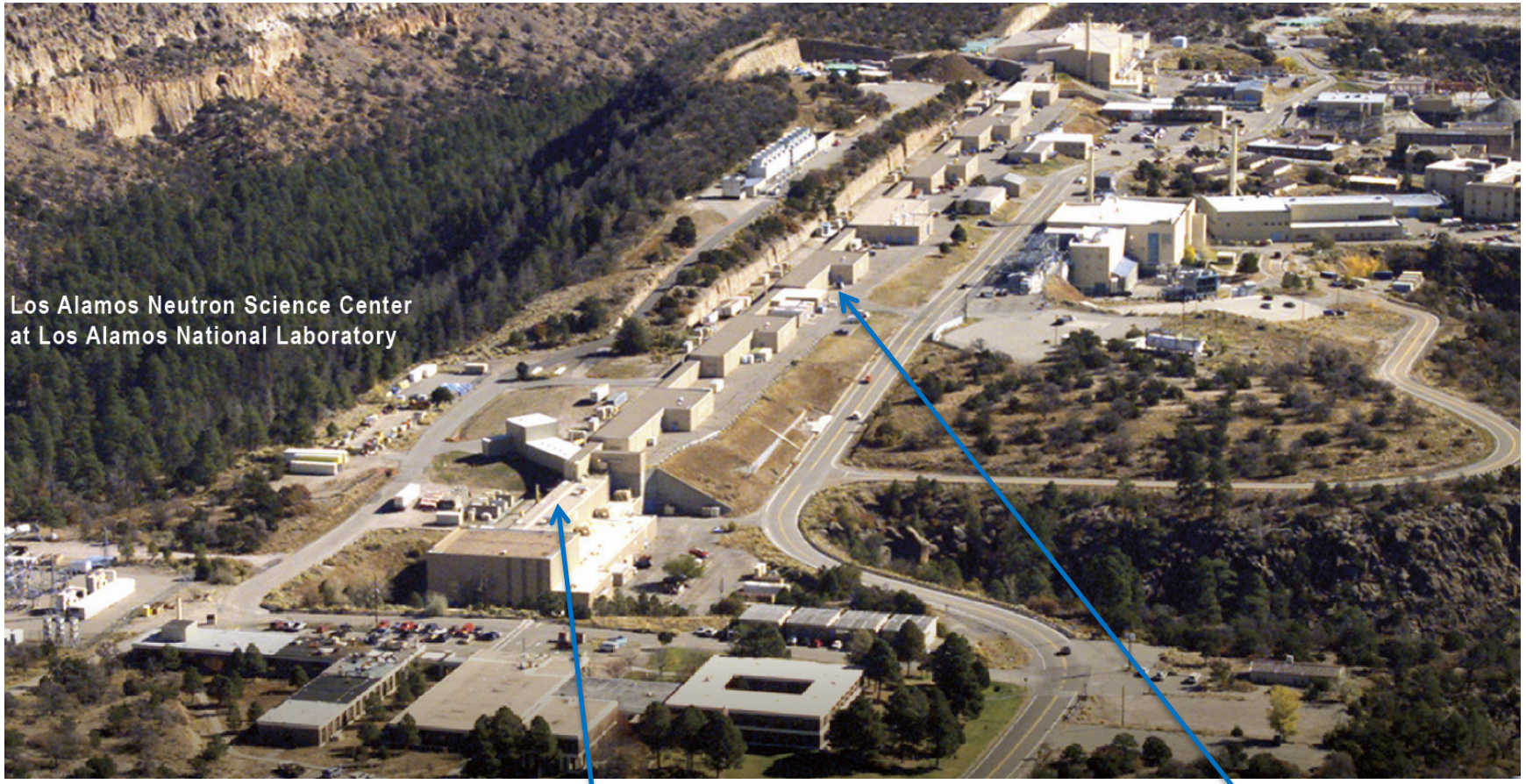

800 m, 800 MeV

Protons (p) and hydrogen ions (H^-)

Drift-tube linac (DTL)

62 m, 0.75-100 MeV

$\beta = v/c = 0.04\text{-}0.43$

4 201.25-MHz tubes (≤3 MW)

Coupled-cavity linac (CCL)

731 m, 100-800 MeV

$\beta = v/c = 0.43\text{-}0.84$

44 805-MHz klystrons (1 MW)

LANSCE Accelerating Structures

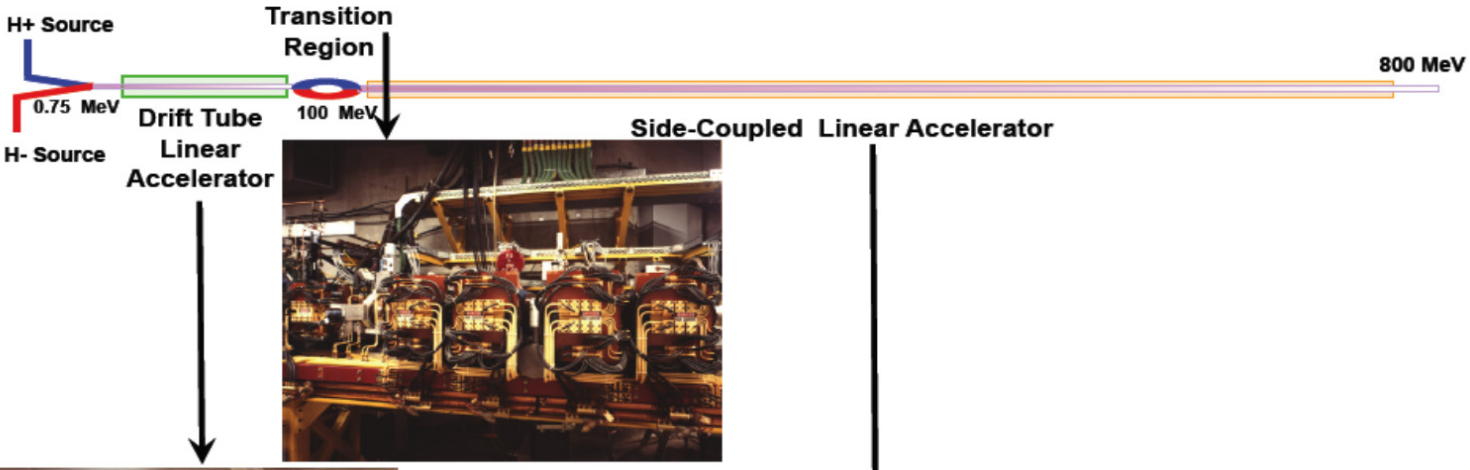

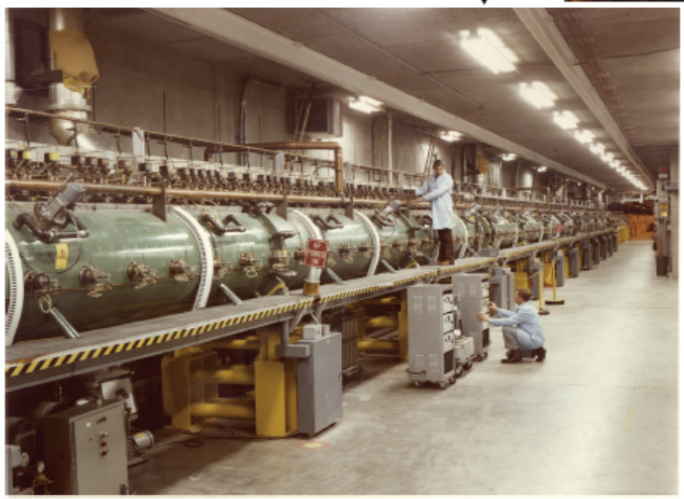

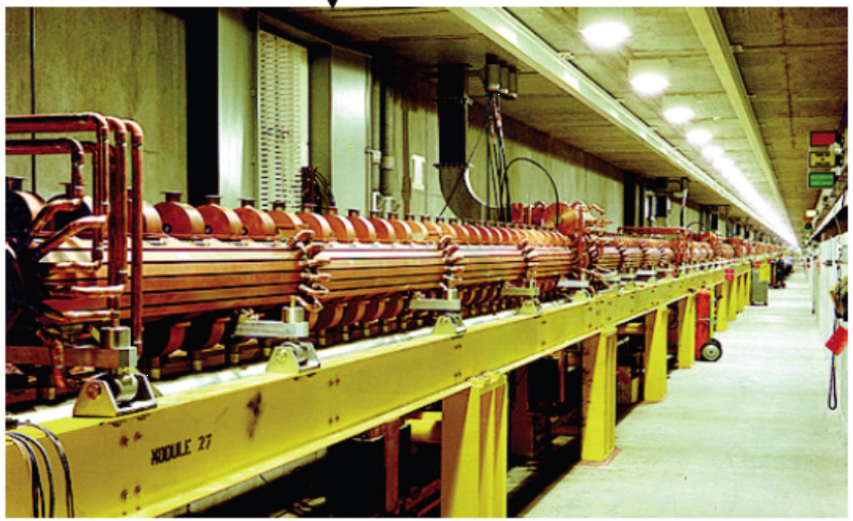

Los Alamos
NATIONAL LABORATORY
EST. 1943

Operated by the Los Alamos National Security, LLC for the DOE/NNSA

NNSA

Induction Accelerator

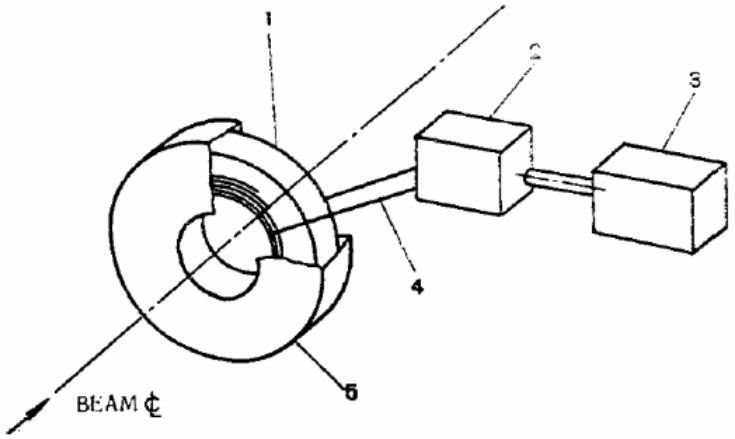

Fig. 1. Induction accelerator principle:
1 — laminated iron core; *2* — switch; *3* — pulse forming network; *4* — primary loop; *5* — secondary (case).

$$\oint \vec{E} \cdot \vec{dl} = -\frac{1}{c} \int_S \frac{\vec{dB}}{dt} \cdot \vec{ds},$$

Table 3. Parameters for Typical Induction Accelerators

Accelerator	Astron Injector Livermore 1963	ERA Injector Berkeley 1971	NEP 2 Injector Dubna 1971	ATA Livermore 1983
Kinetic energy, MeV	3.7	4.0	30	50
Beam current on target, A	350	900	250	10,000
Pulse duration, ns	300	2-45	500	50
Pulse energy, kJ	0.4	0.1	3.8	25
Rep rate, pps	0-60	0-5	50	5
Number of switch modules	300	17	750	200

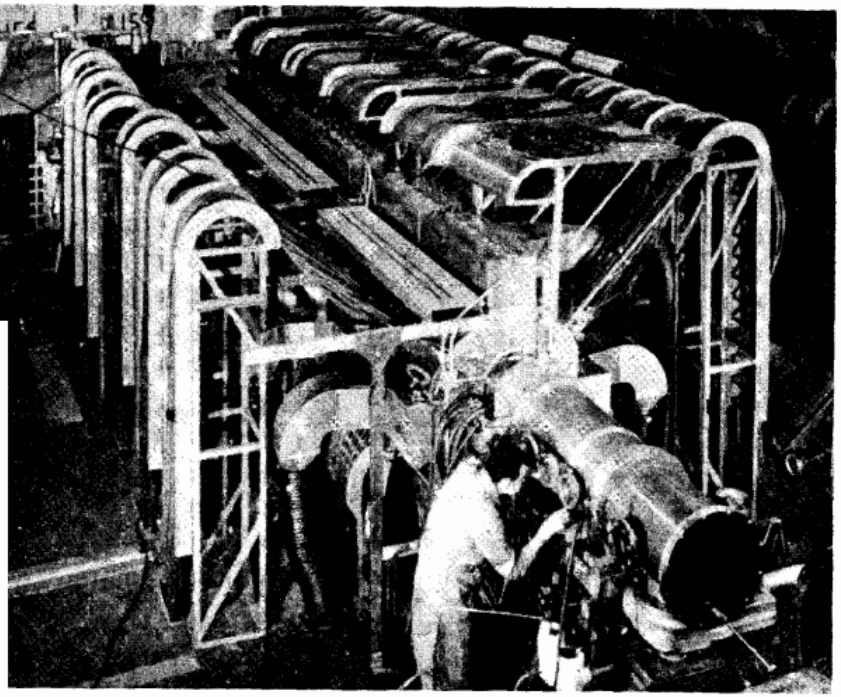

Overhead view of the Astron accelerator as it appeared when first put into operation.

DARHT at LANL – two linear induction accelerators

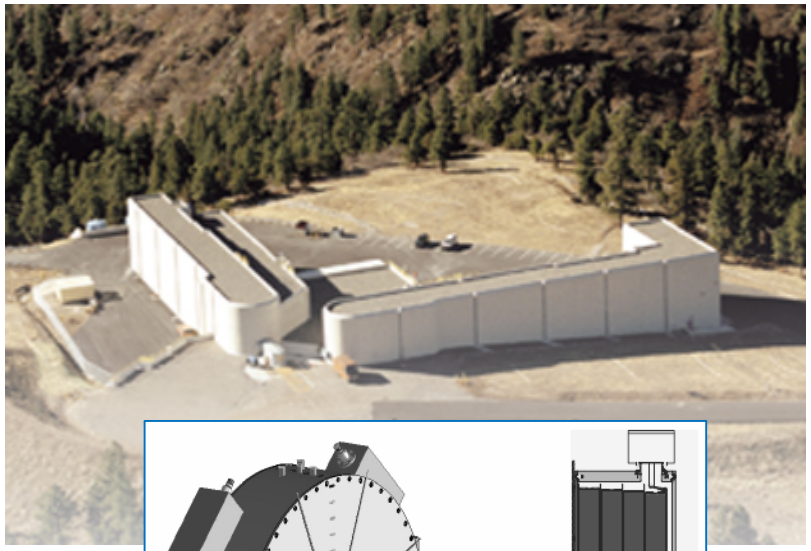

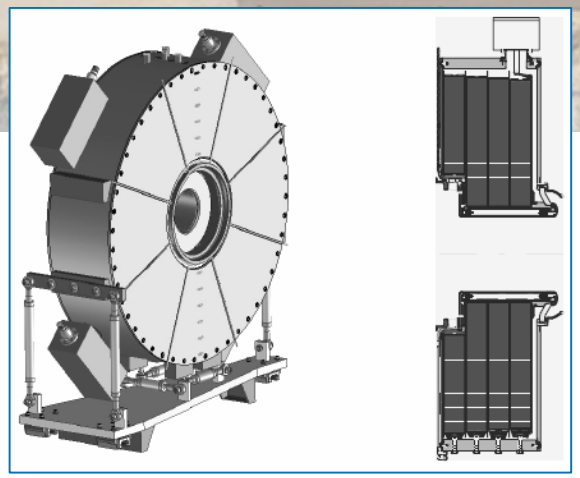

Induction cells of Axis 2:
Beam pipe diameter 12" (8 cells) and 10" (66 cells)

Dual-Axis Radiographic Hydrodynamic Test (DARHT) facility:

- Axis 1 (1999): 60-ns pulse, 2 kA, 20 MeV e-beam → high-Z target → X-rays (64 cells)
- Axis 2 (2008): 1.6-μs long flat-top pulse (4 short pieces cut), 2 kA, 17 MeV (74 cells)

Resonance acceleration principle

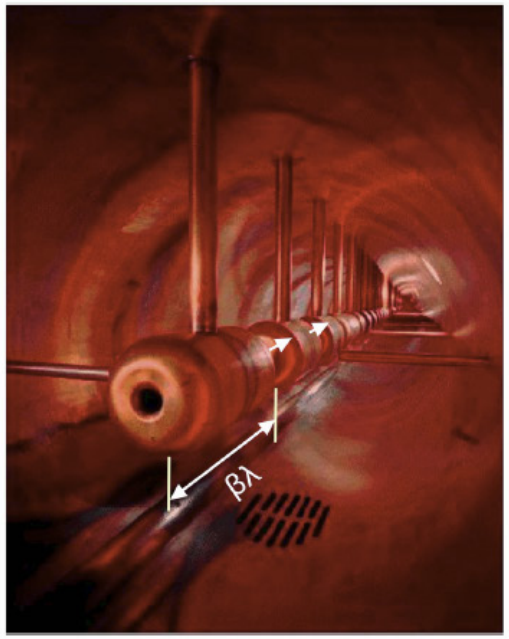

Alvarez accelerating structure

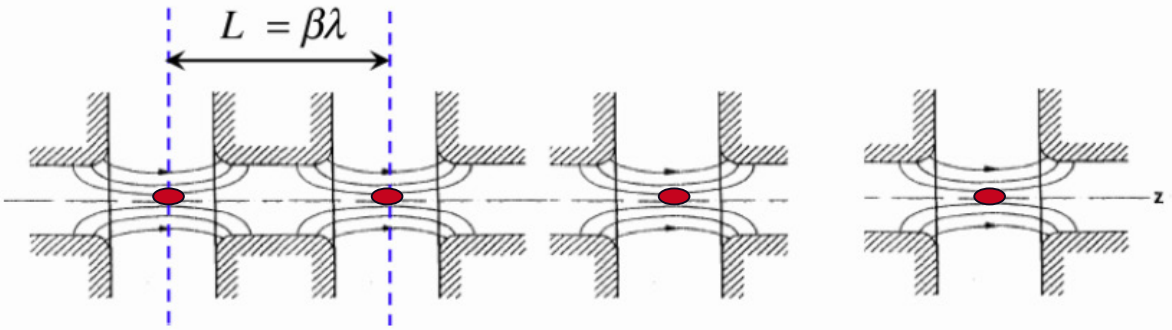

Field distribution in RF structure: $E_z(z,r,t) = E_g(z,r)\cos(\omega t)$

Time of flight between RF gaps $t_{flight} = T_{RF\ period} = \frac{1}{f}$

Distance between RF gaps $L = n\beta c T_{RF\ period} = n\beta\lambda$

RF Frequency f

- Synchronism between the accelerating field and particles is due to the linac spatial structure: particles arrive at the gaps when the electric field is in the accelerating phase, and are hidden from the field inside drift tubes during the decelerating phase.
- The above example is a 0-mode accelerating structure (Alvarez DTL): the gap fields work in phase, $\Delta\varphi = 0$. BTW, $t_{flight} = mT_{RF}$, where $m = 2,3,\ldots$ will work too ($m\beta\lambda$-mode).

Resonance acceleration: π-mode

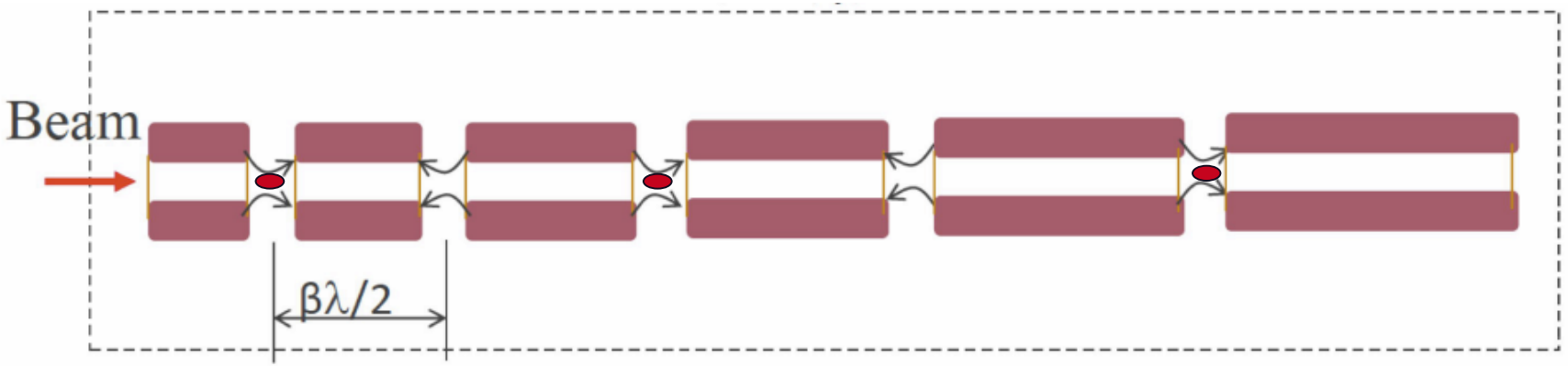

Accelerating structure with π - type standing wave.

- This is a π-mode accelerating structure (e.g., Wideroe DTL): the fields in the adjacent gaps are in opposite phases, $\Delta\varphi = \pi$.
- Particles accelerated in a gap should arrive to the next gap in one half of the RF period (strictly speaking, $(n+1/2)T_{RF}$) so that its electric field changes to the accelerating phase.
- Still there is a “synchronism” between the RF field and the linac spatial structure.

Example: Inter-digital H-mode (IH) structure

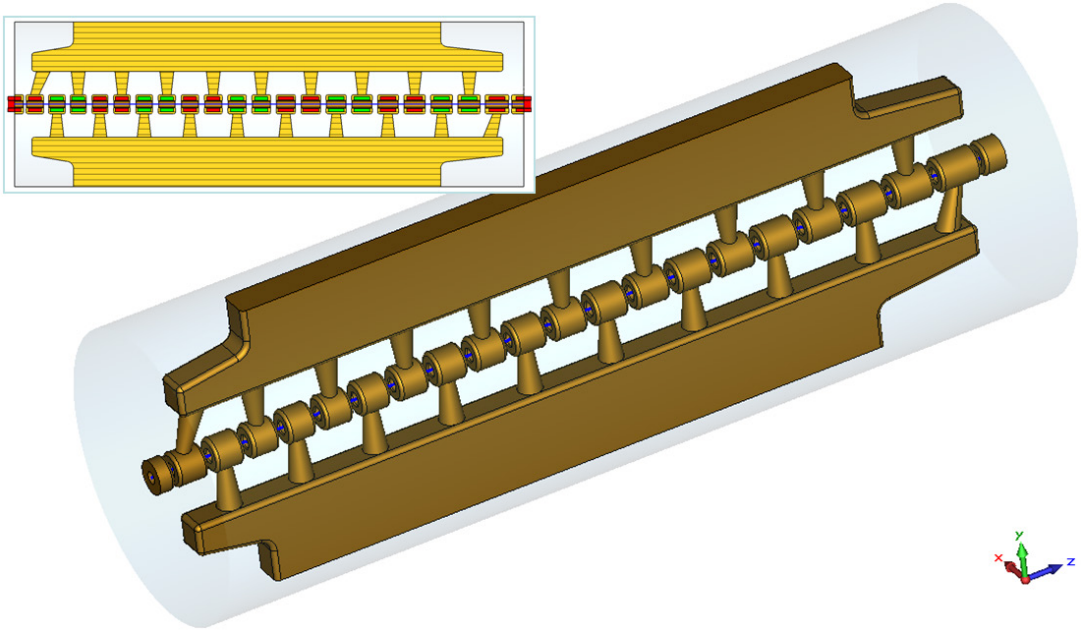

IH-PMQ structure for deuterons from $\beta=v/c$=0.04 to 0.055:
f=201.25 MHz, I=50 mA
L=73.5 cm, a=0.5-0.55 cm.
CST Studio simulations: RF fields (MWS), PM quadrupole fields (EMS), and beam dynamics (Particle Studio).

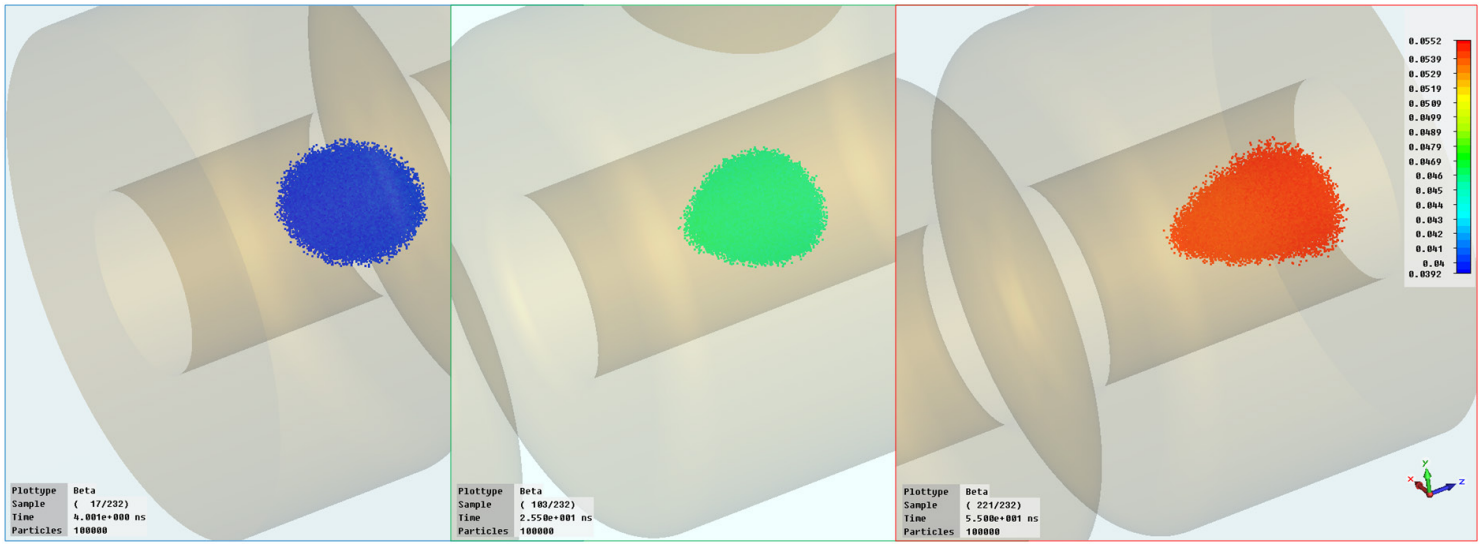

Inter-digital H-mode (IH) structure

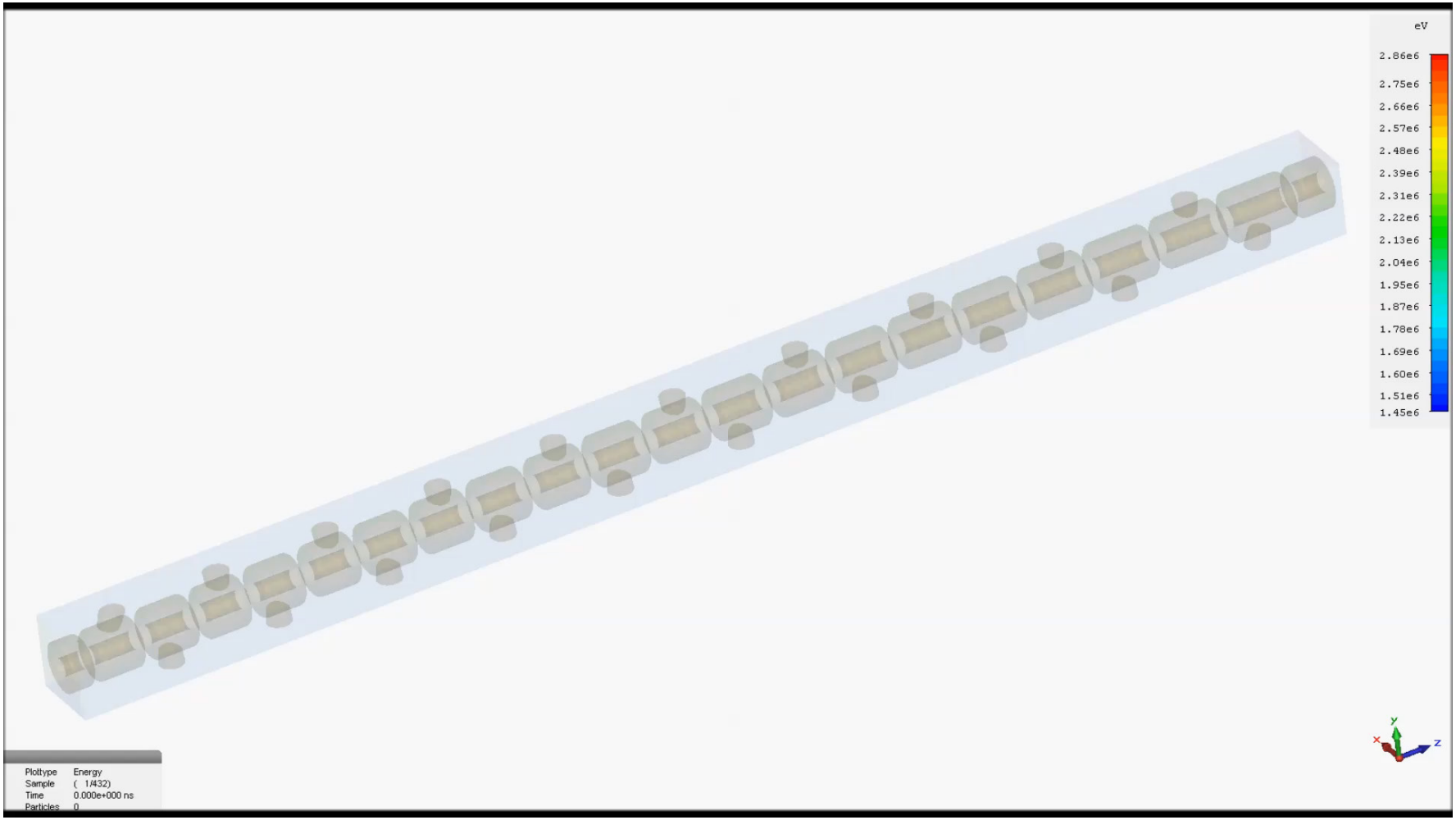

10 bunches of 10K particles are accelerated in the cavity

Accelerating gap and transit-time factor - 1

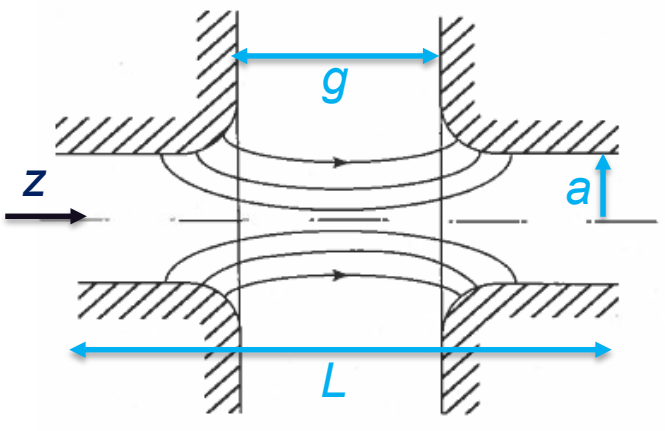

$$\frac{d\vec{r}}{dt} = \vec{v}; \quad \frac{d\vec{p}}{dt} = q(\vec{E} + \vec{v} \times \vec{B})$$

On-axis longitudinal electric field ($\omega = 2\pi f$ - RF)

$$E_z(z,t) = E(z)\cos(\omega t + \varphi)$$

The particle energy gain in the gap (t=0, z=0 – center)

$$\Delta W = \int_{-L/2}^{L/2} F_z dz = q \int_{-L/2}^{L/2} E_z(z, t(z)) dz,$$

where $t(z) \cong z / v_z \cong z / (\beta c)$. (!) Then we rewrite

$\Delta W = qV_0 T \cos\varphi$, where $V_0 \equiv \int_{-L/2}^{L/2} E_z(z) dz$ is the gap voltage, and T is called the transit-time factor:

$$T \equiv \frac{1}{V_0}\left[\int_{-L/2}^{L/2} E_z(z)\cos\frac{\omega z}{\beta c} dz - \tan\varphi \underbrace{\int_{-L/2}^{L/2} E_z(z)\sin\frac{\omega z}{\beta c} dz}_{=0}\right].$$

(definition of the gap center)

Accelerating gap and transit-time factor – 2

The average accelerating field of a cell is defined as $E_0=V_0/L$, and product E_0T is called accelerating gradient. The particle energy gain in the gap

$$\Delta W = qE_0TL\cos\varphi.$$

The transit-time factor shows the efficiency of energy gain by particle crossing the gap. In the case of static field T=1.

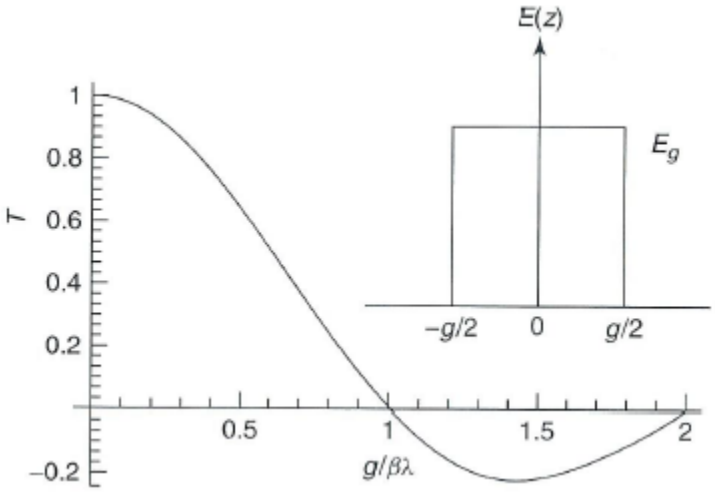

Note $\omega/c = 2\pi f/c = 2\pi/(cT_{RF}) = 2\pi/\lambda = k,$

where λ is the RF wavelength. Then on axis

$$T(r=0) = \frac{1}{V_0}\int_{-L/2}^{L/2} E_z(0,z)\cos\frac{2\pi z}{\beta\lambda}dz.$$

Example: constant field $E_z(z)=E_g$ in the gap

$$T = \sin\frac{\pi g}{\beta\lambda}\Big/\left(\frac{\pi g}{\beta\lambda}\right).$$

Accelerating gap and transit-time factor – 3

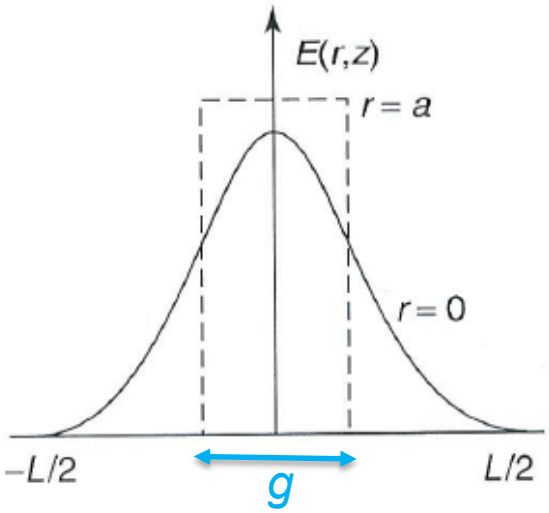

The transit-time factor and energy gain depend on the particle radial position when it crosses the gap. For particles off axis, at radius *r*

$$T(r) = \frac{1}{V_0}\int_{-L/2}^{L/2} E_z(r,z)\cos\frac{2\pi z}{\beta\lambda}dz.$$

In axisymmetric case, using the RF field expansion in cylindrical coordinates, one can show that

$$T(r) = T(0)I_0\left(\frac{2\pi}{\gamma\beta\lambda}r\right),$$

where $I_0(x)$ is the modified Bessel function. For $x<<1$, $I_0(x) = 1+x^2/4+\ldots$ This means that off-axis particles gain a bit more energy passing through the gap.

(return to IH-PMQ picture)

Synchronous particle and RF phase

A particle that arrives from one gap (cavity) to the next one in exactly one RF period is called synchronous. It will see the same RF phase φ_s – synchronous phase.

On-axis longitudinal electric field $E_z(z,t) = E(z)\cos(\omega t + \varphi_s)$, and its energy gain is $\Delta W_s = qE_0TL\cos\varphi_s$. When φ_s=0, the field is max at t=0: the particle arrives at the gap center on crest. This is typical for electron linacs.

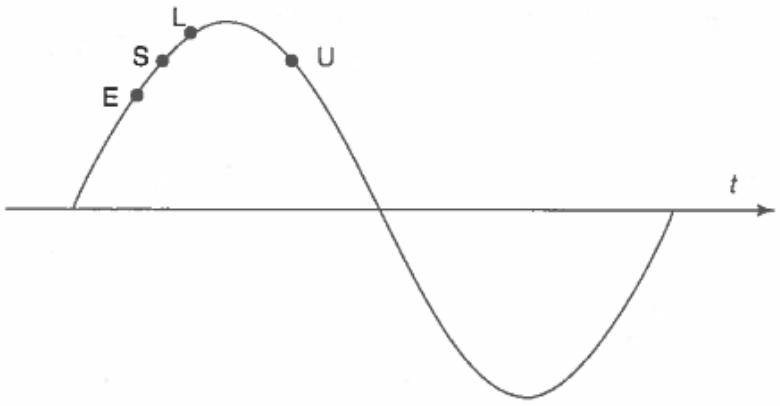

When φ_s=-π/2, no acceleration, only beam bunching.

For proton / ion linacs the synchronous RF phase φ_s is usually <0. Cf. phase focusing (auto-focusing mechanism):

An earlier particle (E) receives smaller energy kick than the synchronous one (S); it will arrive a bit later to the next gap. A later particle (L) receives larger energy gain, so it will catch up with S. This results in stable longitudinal oscillations around synchronous particle. U corresponds to unstable phase.

Since $dW = mc^2 d\gamma = mc^2\beta\gamma^3 d\beta$, the synchronous particle velocity change in gap n is $\beta_{n+1} \cong \beta_n + \dfrac{qE_0TL}{mc^2\beta_s\gamma_s^3}\cos\varphi_s$. It makes sense to set $\beta_s = (\beta_{n+1} + \beta_n)/2$.

Buncher cavities

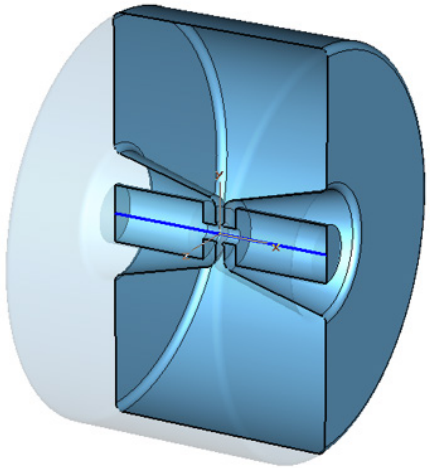

a.

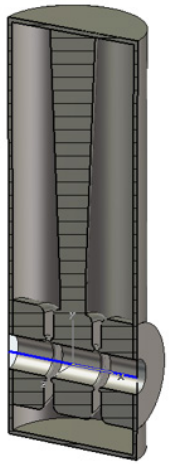

b.

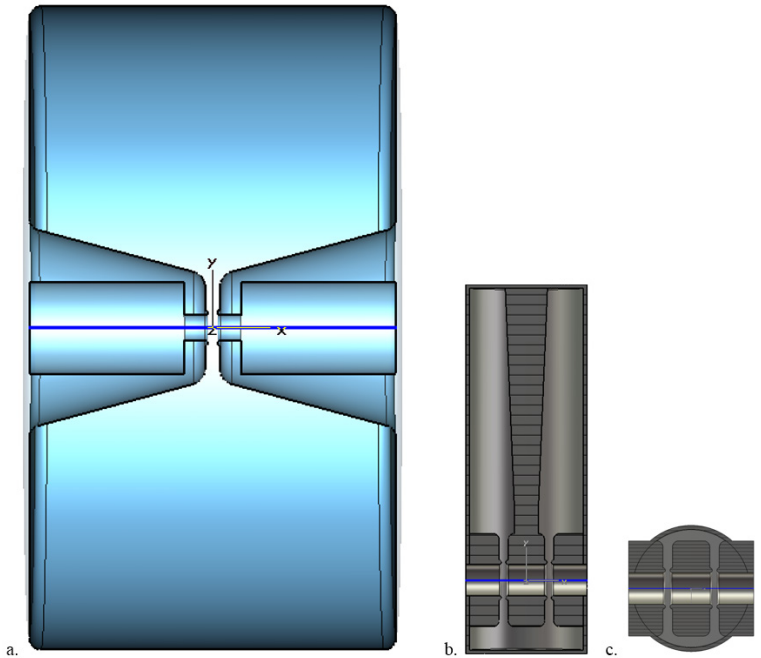

a. b. c.

Two buncher cavities: (a) re-entrant and (b) coaxial quarter-wave (λ/4) types. Right – on the same scale.

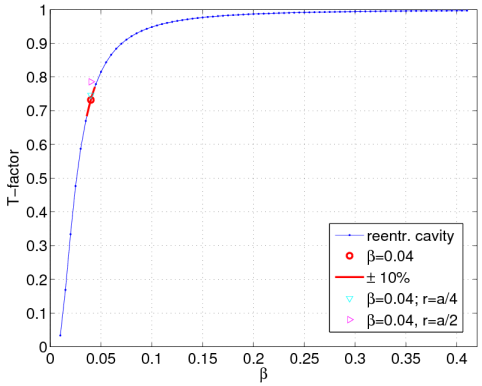

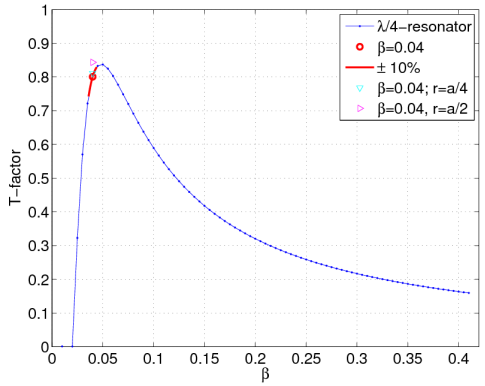

Transit-time factors for two cavities vs velocity

Standing wave vs traveling wave

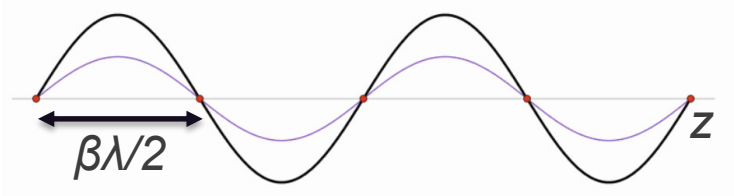

A particle with velocity βc in z direction will be synchronous in the standing wave with wave number $k_z = \frac{2\pi}{\beta\lambda}$.

The standing wave can be considered as a sum of two waves traveling in opposite directions:

$$E_0 \cos k_z z \cos \omega t = \frac{E_0}{2}\left[\cos\left(k_z z - \omega t\right) + \cos\left(k_z z + \omega t\right)\right].$$

The phase velocity of the wave traveling in +z direction is equal to the particle velocity:

$$d\varphi = d\left(k_z z - \omega t\right) = 0 \rightarrow v_{ph} = \frac{dz}{dt} = \frac{\omega}{k_z} = \frac{\omega\beta\lambda}{2\pi} = \frac{\beta\lambda}{T_{RF}} = \beta c.$$

It is often convenient to consider an acceleration by an "equivalent" traveling wave: in axisymmetric case

$$E_z = EI_0\left(\frac{k_z r}{\gamma}\right)\cos\varphi, \text{ where } E = E_0 T;$$

$$E_r = -\gamma EI_1\left(\frac{k_z r}{\gamma}\right)\sin\varphi; \qquad B_\theta = -\frac{\beta\gamma}{c}EI_1\left(\frac{k_z r}{\gamma}\right)\sin\varphi;$$

Synchrotron oscillations and separatrix

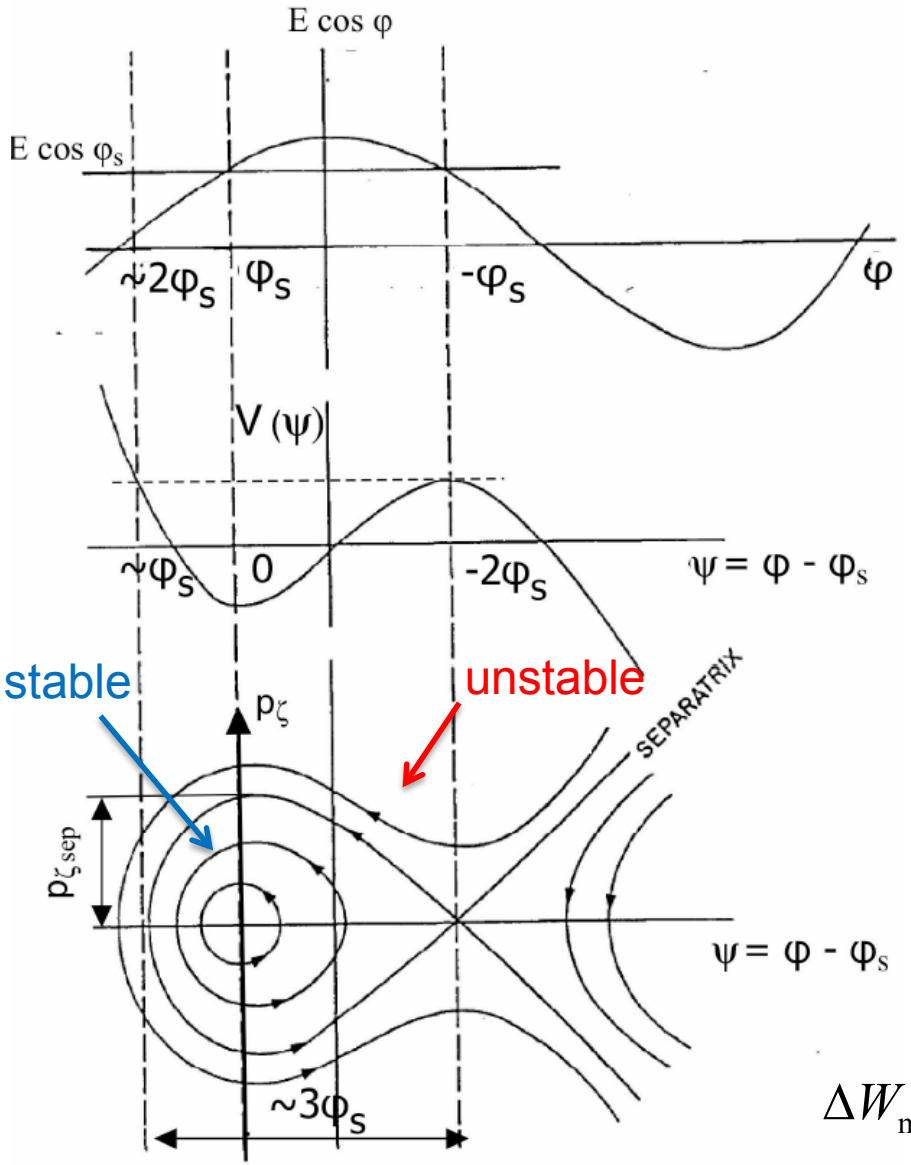

Phase oscillations around synchronous particle are stable inside the separatrix. Its phase width is $\Delta\psi \cong 3\,|\,\varphi_s\,|,\ \varphi_s < 0.$

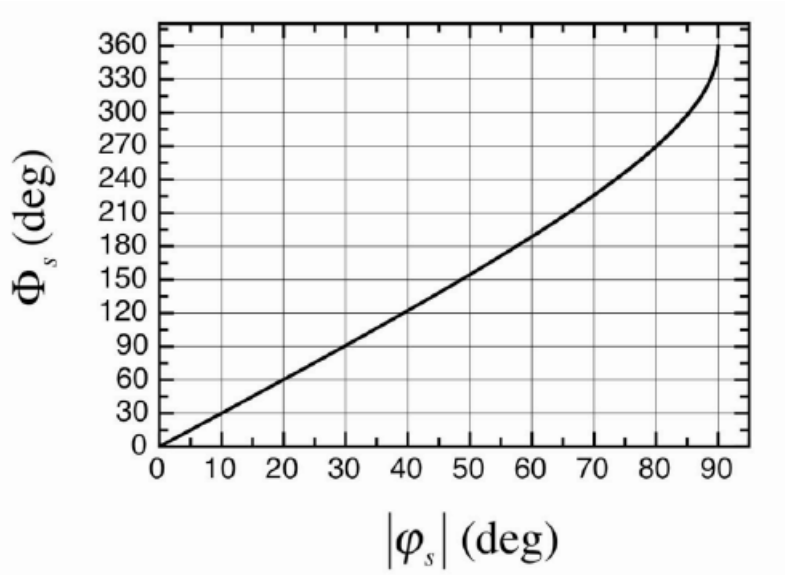

Phase width of separatrix as a function of synchronous phase.

The separatrix energy width max at $\varphi = \varphi_s$

$$\Delta W_{\max} = \sqrt{2qE_0Tmc^2\beta_s^3\gamma_s^3\left(\varphi_s\cos\varphi_s - \sin\varphi_s\right)/\pi}.$$

Acceleration in structures with higher β

In ion linacs at low beam velocities, the synchronism is achieved by changing the cell lengths: $L_c \sim \beta\lambda$. At higher energies, usually $\beta>0.5$, structures with blocks of identical cells $\beta = \beta_g$ are more cost efficient.

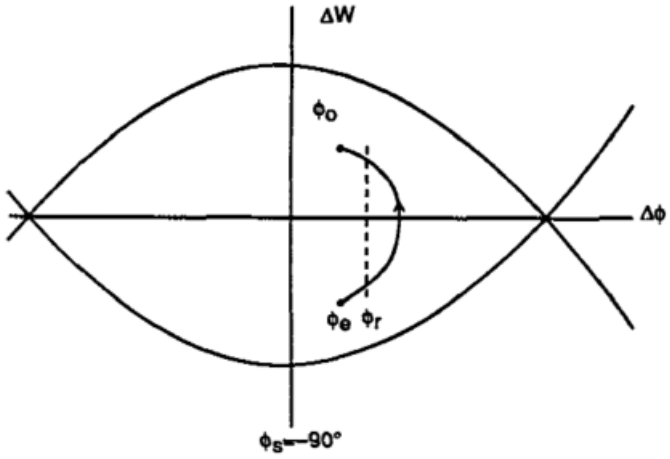

Here $\cos\varphi_r = <\cos\varphi_i>$. Particle starts with $\varphi<\varphi_r$. The phase moves up above φ_r in the 1st half, then down below φ_r.

Phase space trajectory in structure with constant length cell

Because cell lengths are equal, actual synchronous phase $\varphi_s = -90^o$. Energy gain per tank:

$$\Delta W_{ref} = qE_o T \cos\varphi_{ref} N_{cell} \frac{\beta\lambda}{2}$$

For electrons $v \approx c$ starting at rather low energies, ~MeV, practically in the source (electron gun). No problem of synchronism; acceleration on crest ($\cos\varphi=1$). Still there is transverse RF defocusing, so focusing quads are needed.

RF defocusing

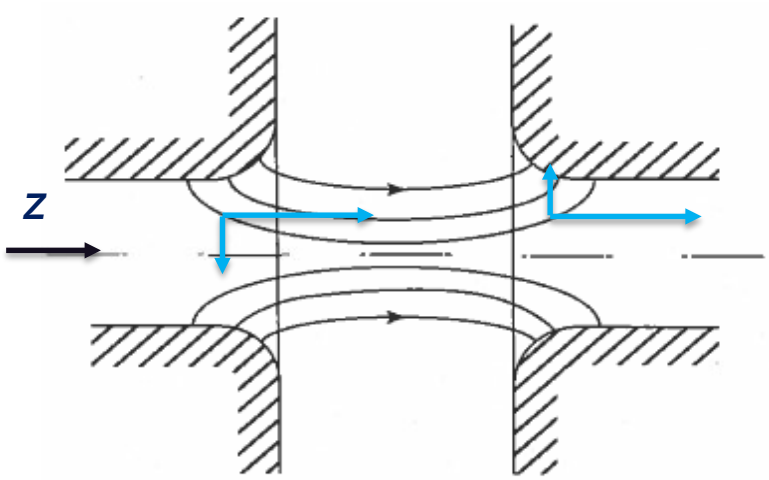

The transverse component of the electric field deflects off-axis particles at the gap entrance and exit. In ion linacs, the requirement of longitudinal stability ($\varphi_s<0$) leads to a net deflection: the particle receives a larger transverse kick at the exit than at the entrance, due to the rising field. This is a result of a rather general Earnshaw's theorem (from Laplace eq.).

In the particle rest frame, the RF fields become electrostatic, hence for potential *U*

$$\Delta U = \partial_x^2 U + \partial_y^2 U + \partial_z^2 U = 0.$$

Stability in *i* direction requires $\partial_i^2 U > 0,\ i = x, y, z$. This means that the RF focusing cannot be achieved in all three directions simultaneously.

There is a way around: alternating $\varphi_s<0$ and $\varphi_s>0$ in adjacent gaps (cells). This provides (longitudinal focusing + transverse defocusing) and (longitudinal defocusing + transverse focusing) alternatively – Alternating-Phase Focusing scheme (works for low currents only!).

The most common method to achieve transverse focusing in linacs in addition to the longitudinal one is to use external magnetic lenses – quadrupoles or solenoids.

Detour: grid / foil transverse focusing

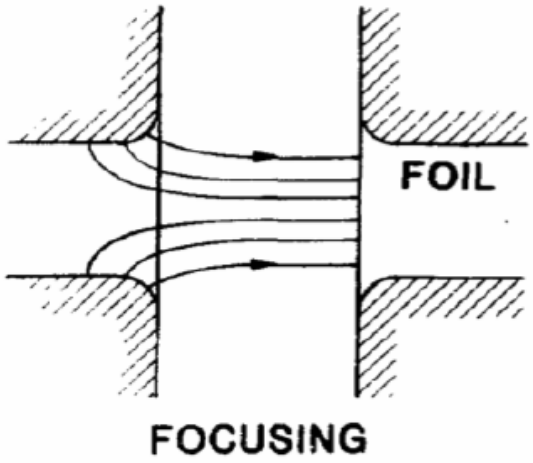

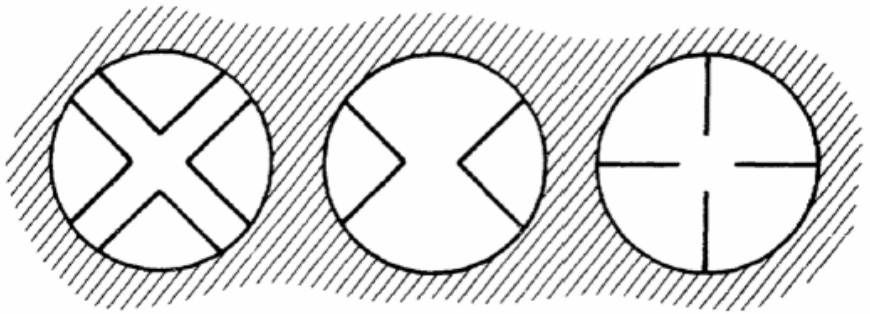

Fig. 7. Various shapes of grids.

RF defocusing effect is suppressed by closing the drift-tube hole at the gap exit with a foil thin enough to be crossed by particles, or by a wire grid.
First test: 1947, Alvarez linac. Obvious limitation – only for low currents.

Quadrupole transverse focusing

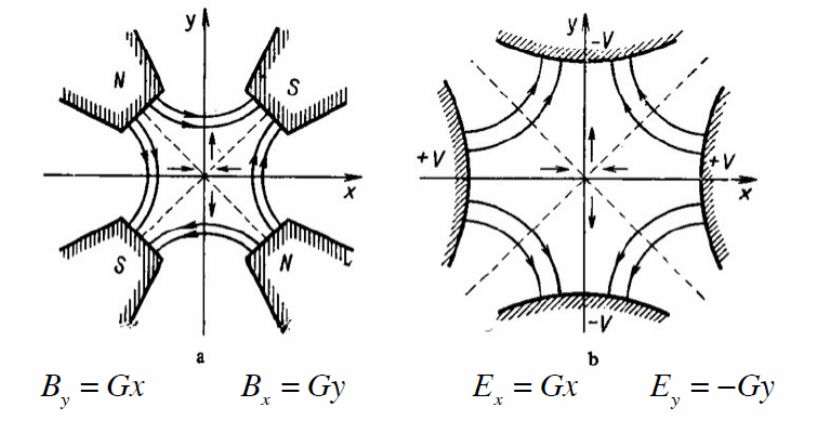

(a) Magnetic quadrupole and (b) electric quadrupole.

Arrows indicate direction of the Lorentz force acting on a positively charged particle moving through the screen toward us. The field is proportional to distance from axis.

The iron poles of ideal quadrupoles are hyperboles in *x*-*y* plane, e.g.

$$2xy = \pm a^2,$$

for magnetic one, where *a* is the radius of the quadrupole aperture.

Quadrupole magnetic fields focus particles transversely on one plane (e.g., in *x*) but defocus in the other. *G* is the quadrupole gradient; units 1 T/m = 0.1 kG/cm.

Either electromagnetic (EMQ, picture below) or permanent-magnet quadrupoles (PMQ) are used in linacs, usually between tanks (resonators) or inside drift tubes.

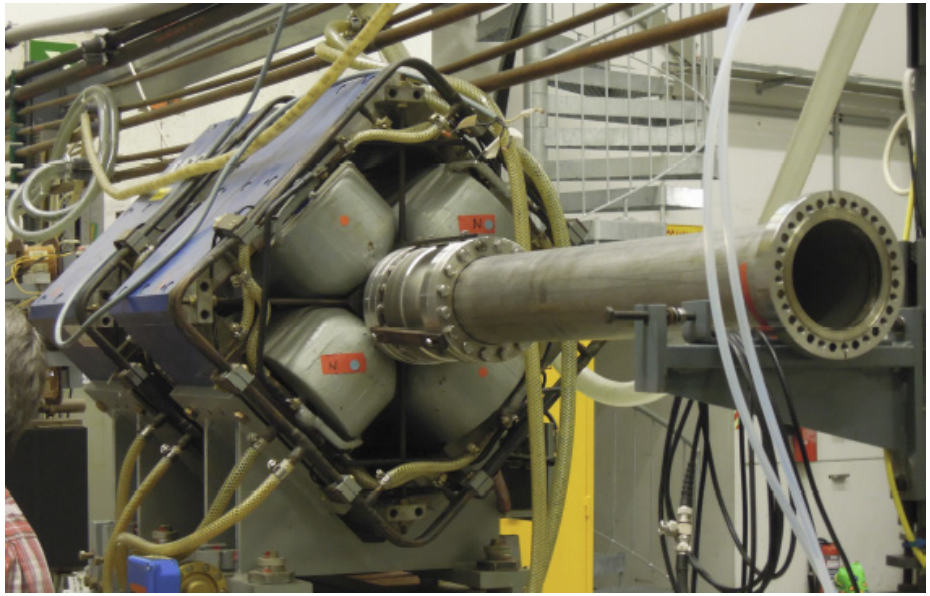

Linac electromagnetic quadrupoles – LANSCE DTL

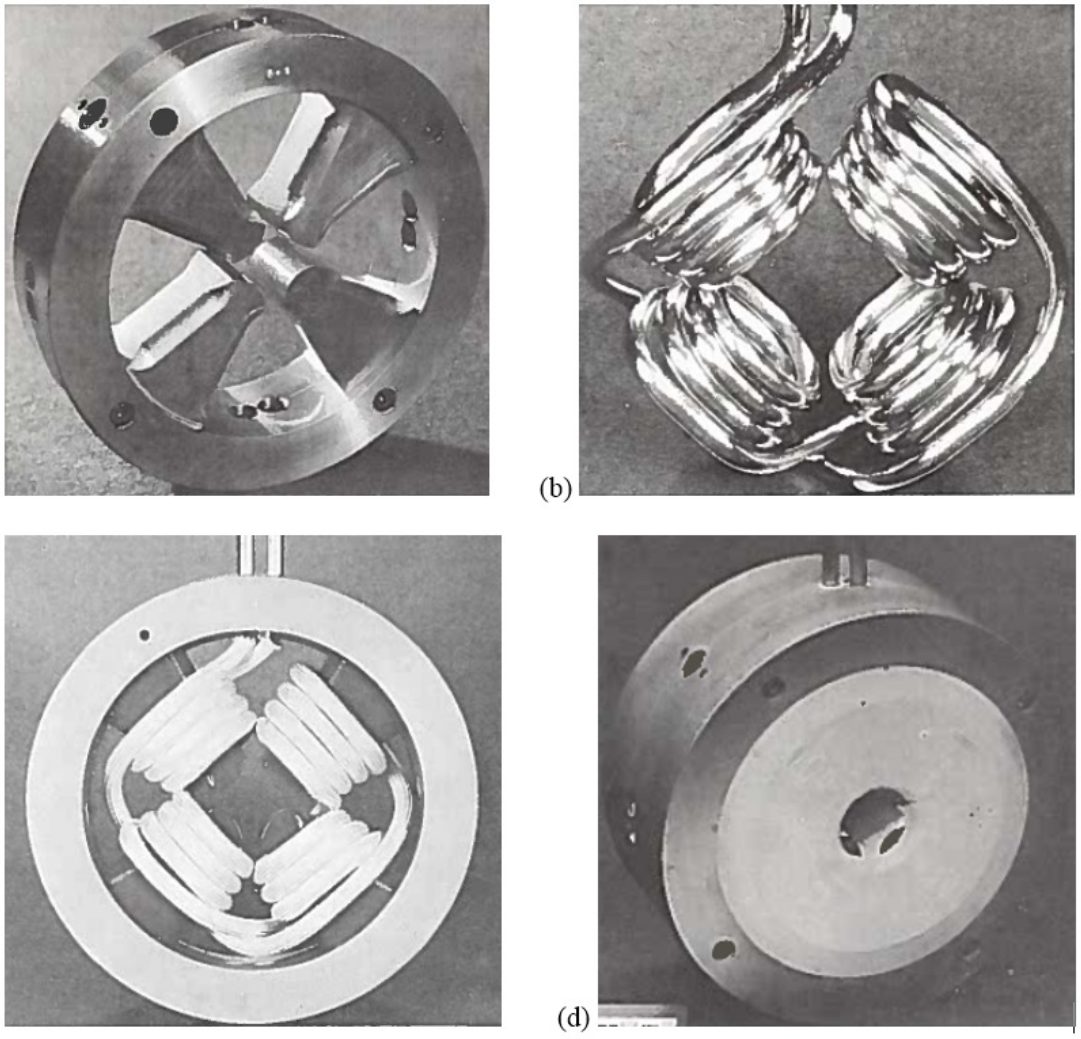

DTL tank 1 EM quadrupoles are installed inside drift tubes:
(a) yoke and pole pieces (iron);
(b) current coil (copper, hollow);
(c) coil assembled with iron;
(d) quadrupole fully assembled.

EM quadrupole gradients are adjusted by changing current: gradient G=73.5 T/m at ~562 A. GL = 2.59 T in Q1.

LANSCE DTL EM quadrupoles – material replacement

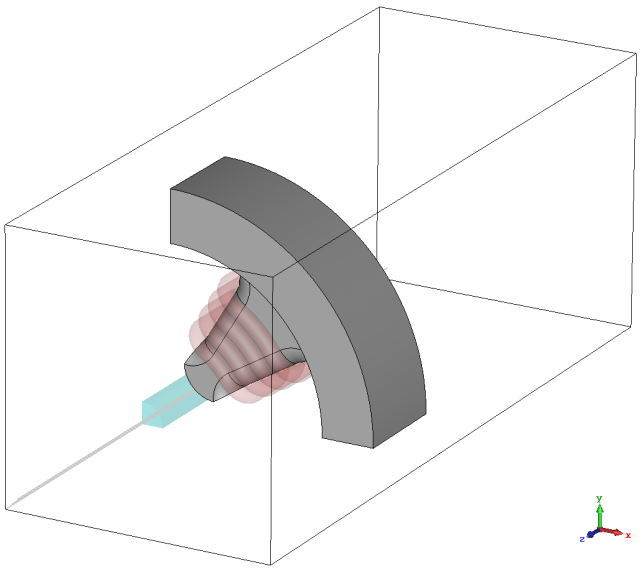

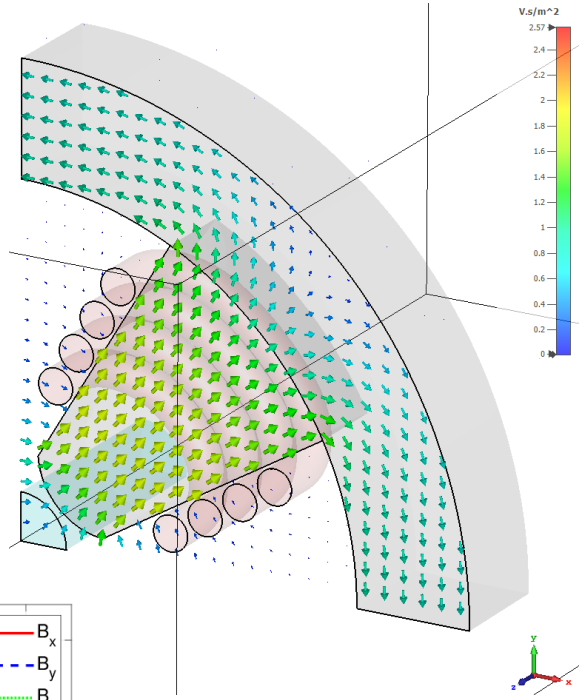

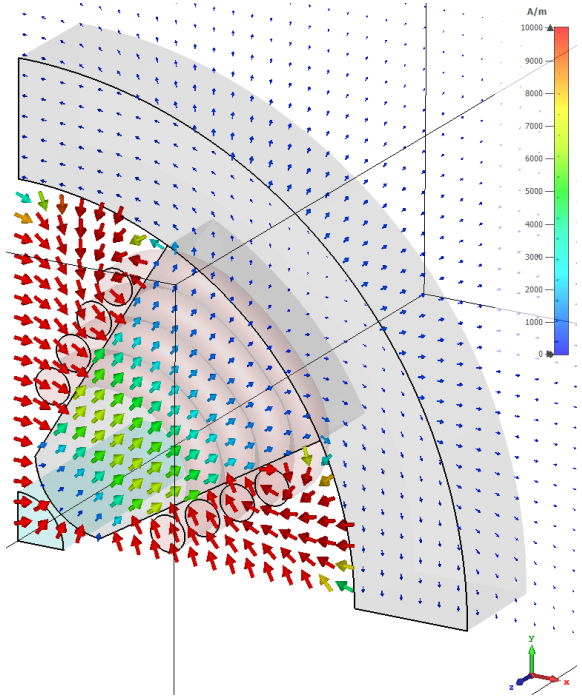

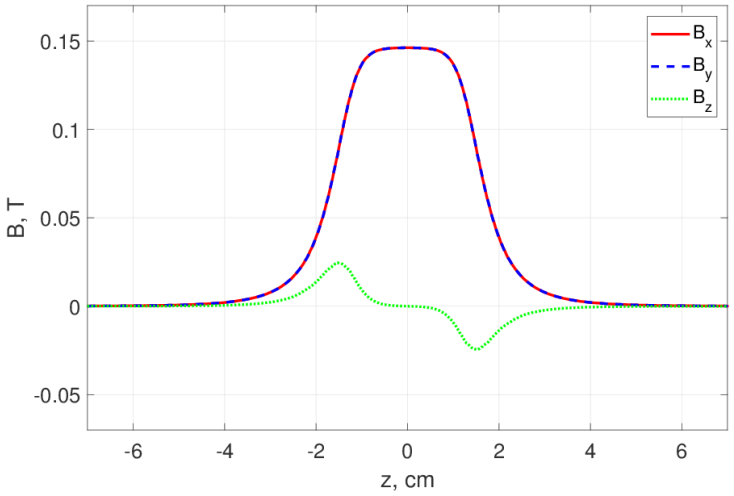

The design strength in Q1 with C1006 steel is achieved at higher current, ~586 A.

Permanent-magnet quadrupoles

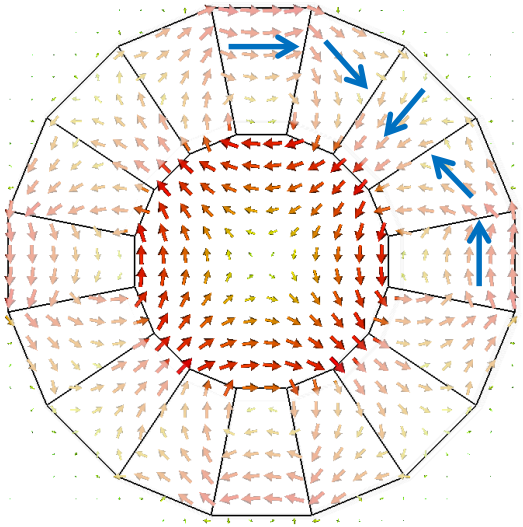

Permanent-magnet quadrupoles are assembled from segments of PM materials, usually SmCo or NdFeB, with properly oriented magnetization vectors in segments. The gradient of such a quadrupole with M = 16 segments (typically M = 12, 16), the remnant field B_r (~1 T), and radii r_{in} and r_{out}, is

$$G = 2B_r\left(\frac{1}{r_{in}} - \frac{1}{r_{out}}\right)K_2; \quad K_2 = \cos^2\frac{\pi}{M}\frac{\sin(2\pi/M)}{2\pi/M} \cong 0.937.$$

Magnetic field in the cross section of M=16 PMQ calculated with CST EM Studio. For r_{in} = 5.5 mm, r_{out} = 11 mm, G= 170 T/m; length L=19 mm.

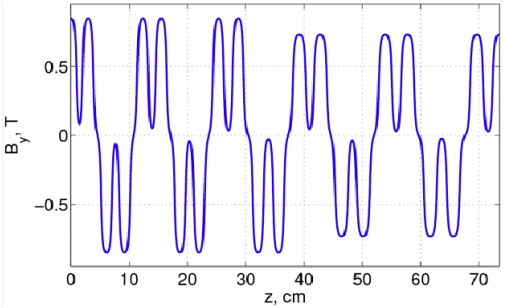

Array of 22 PMQ with FF-DD focusing for IH-PMQ cavity. Notice field overlaps.

Permanent-magnet quadrupoles are installed in the DTL of the Spallation Neutron Source (SNS).

Permanent-magnet quadrupoles in SNS

Cut of the SNS DTL drift tube with PMQ. The bore aperture diameter is 2.5 cm.

Permanent-magnet quadrupoles (PMQ) are installed in the DTL of the Spallation Neutron Source (SNS, Oak Ridge). Now PMQ are also installed in Linac 4 at CERN.

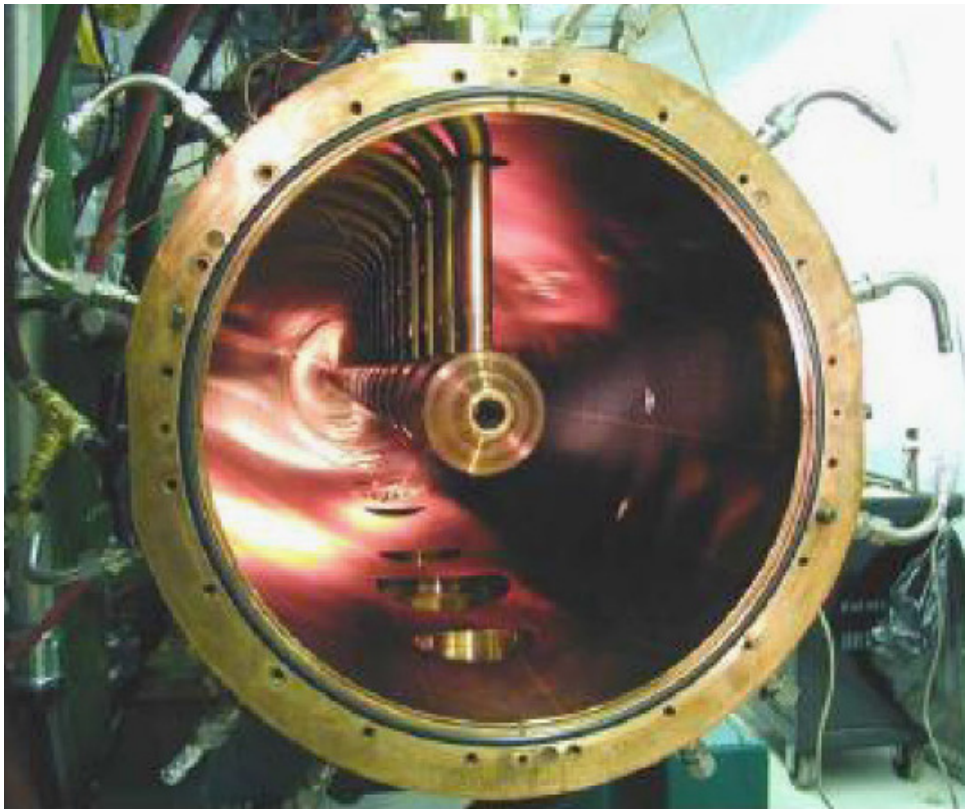

SNS DTL tank 3 with PMQs inside drift tubes (DTs). Some DTs contain beam position monitors (BPM). FFODDO focusing structure.

Quadrupole focusing structures

Quad focusing strength (inverse of focusing length f_q) $\frac{1}{f_q} = \frac{qGL_q}{mc\beta\gamma}$ depends on particle velocity.

The quad gradient $G(z)$ is constant in the middle (G) but decreases near the ends, so its effective length L_q is defined by $GL_q = \int G(z)dz.$

Such a "sharp-edge" approximation is usually sufficient, except when fields overlap.

Various quad focusing structures (period S) are defined by arrangement of elements:

FODO:

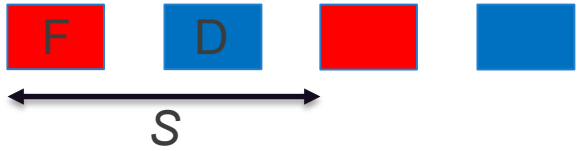

O: drift space. It may include an RF gap.

FOD:

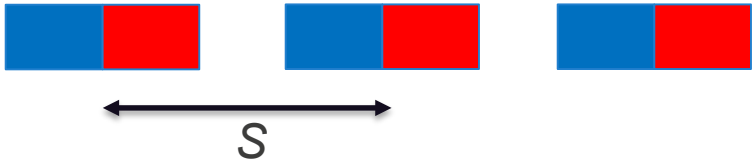

FOF-DOD:

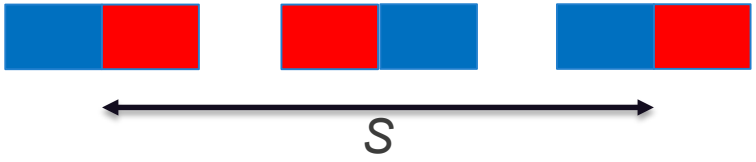

Triplets:

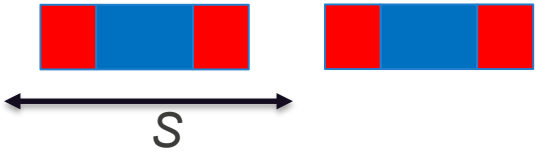

(F/2-D-F/2)

Example: Inter-digital H-mode (IH) structure with PMQ

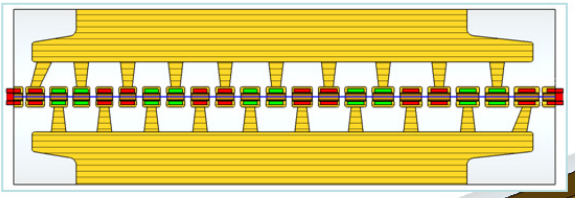

IH-PMQ structure for deuterons from $\beta=v/c=0.04$ to 0.055.
Focusing structure FOFODODO.
CST Particle Studio simulations.

Solenoidal transverse beam focusing

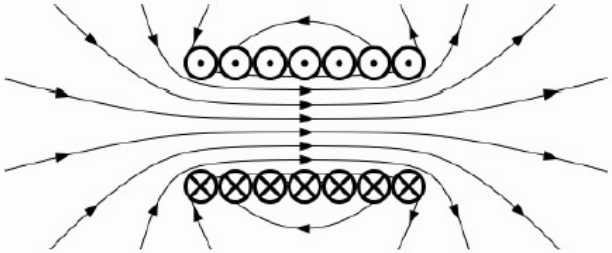

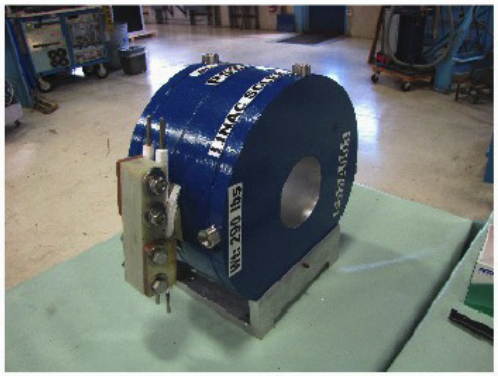

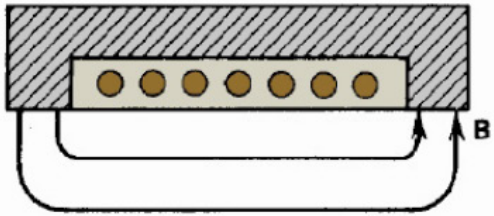

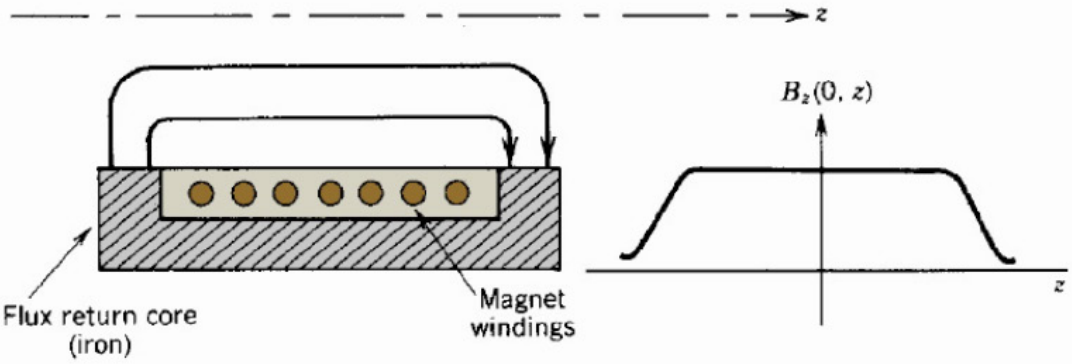

Solenoidal magnetic lens (Humphries, 1999).

FNAL Solenoids

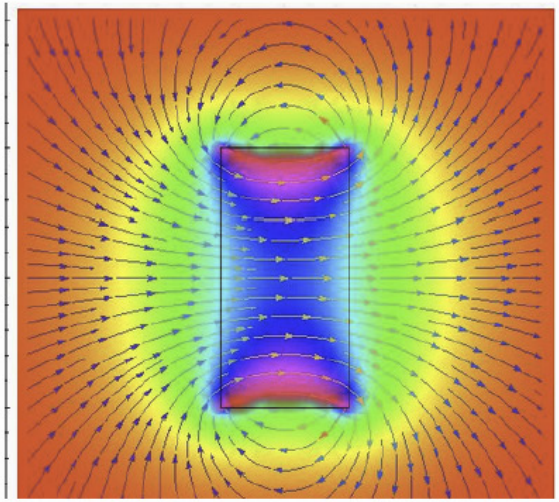

Magnetic field of solenoid

Solenoidal axisymmetric focusing is often used at low beam energies and in heavy-ion linacs between independent superconducting quarter-wave and half-wave cavities.

Electrostatic transverse focusing

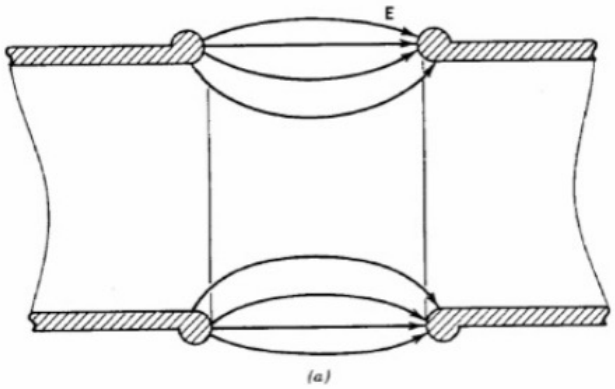

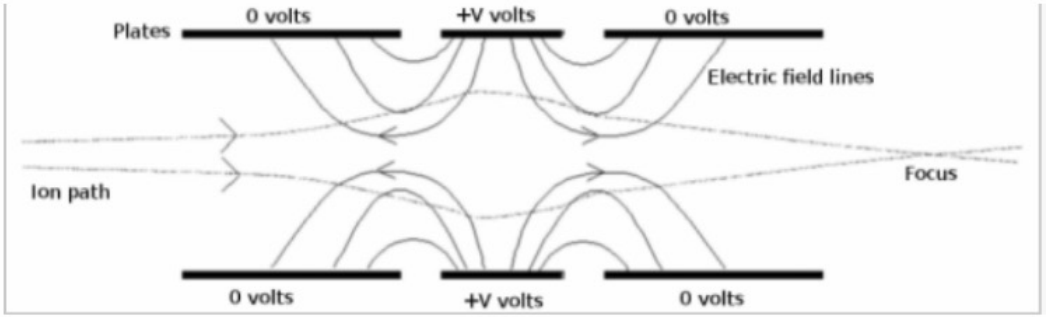

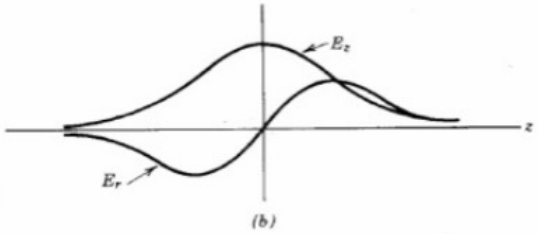

Field distribution in electrostatic lens gap.

Field distribution and particle trajectories in Einzel (equipotential lens).

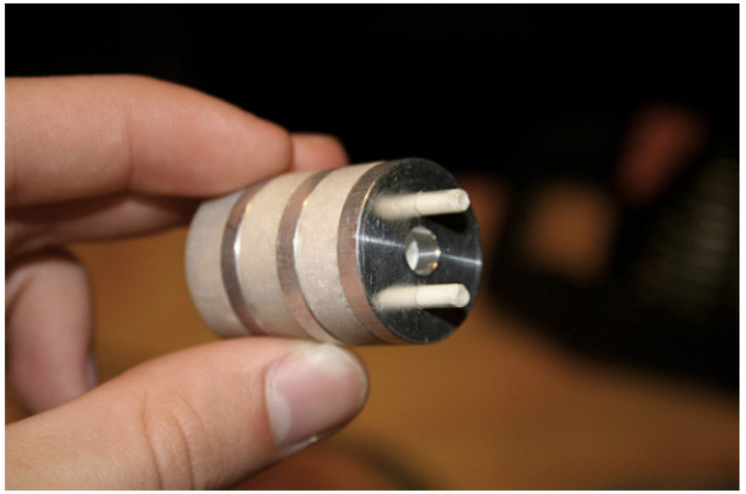

The change of particle slope in a gap

$$\Delta\left(\frac{dx}{dz}\right) = \frac{q}{mc^2}\frac{E_z}{2}\left(\frac{1}{\beta_{out}^2} - \frac{1}{\beta_{in}^2}\right)\left(1 + \frac{x^2}{4L^2}\right)x$$

If $E_z > 0$, then $\beta_{out} > \beta_{in}$ and $\Delta(dx/dz) < 0$,
if $E_z < 0$, then $\beta_{out} < \beta_{in}$ and $\Delta(dx/dz) < 0$.

In both cases, the change of particle slope is negative – the lens is focusing.

Einzel lens in H^- ion source

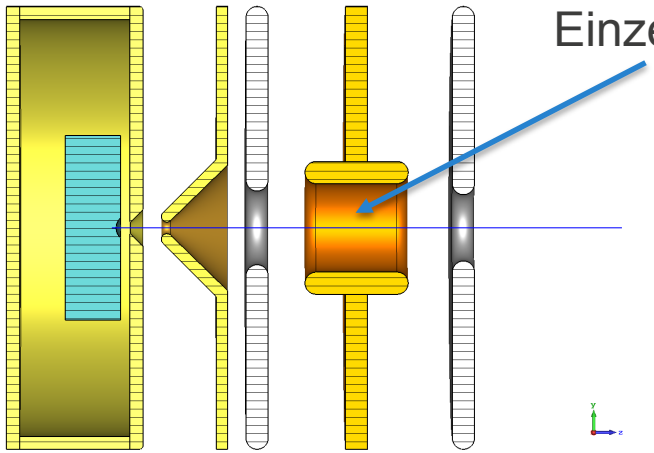

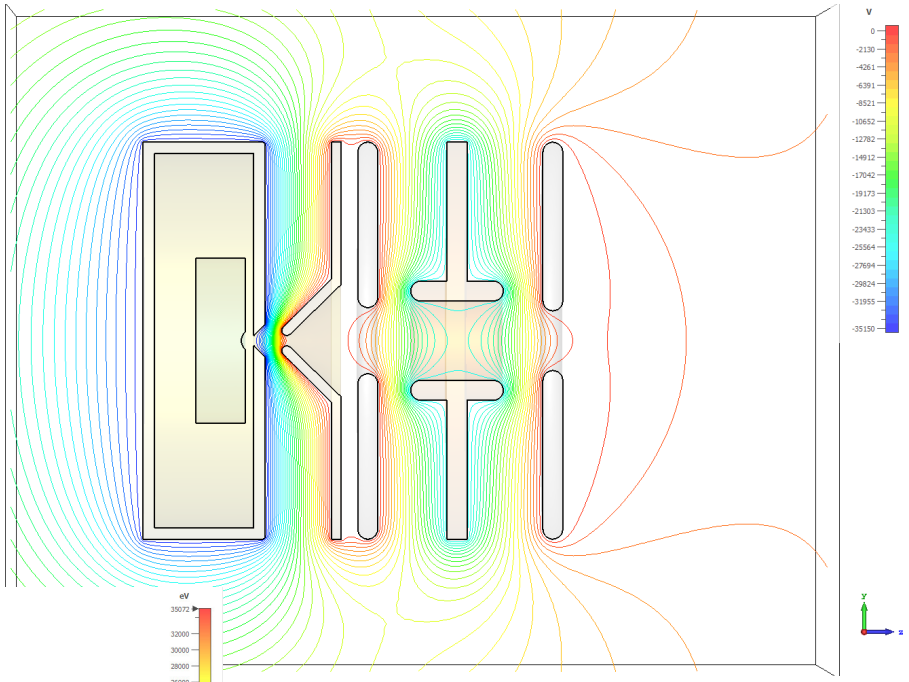

Isolines of electric field

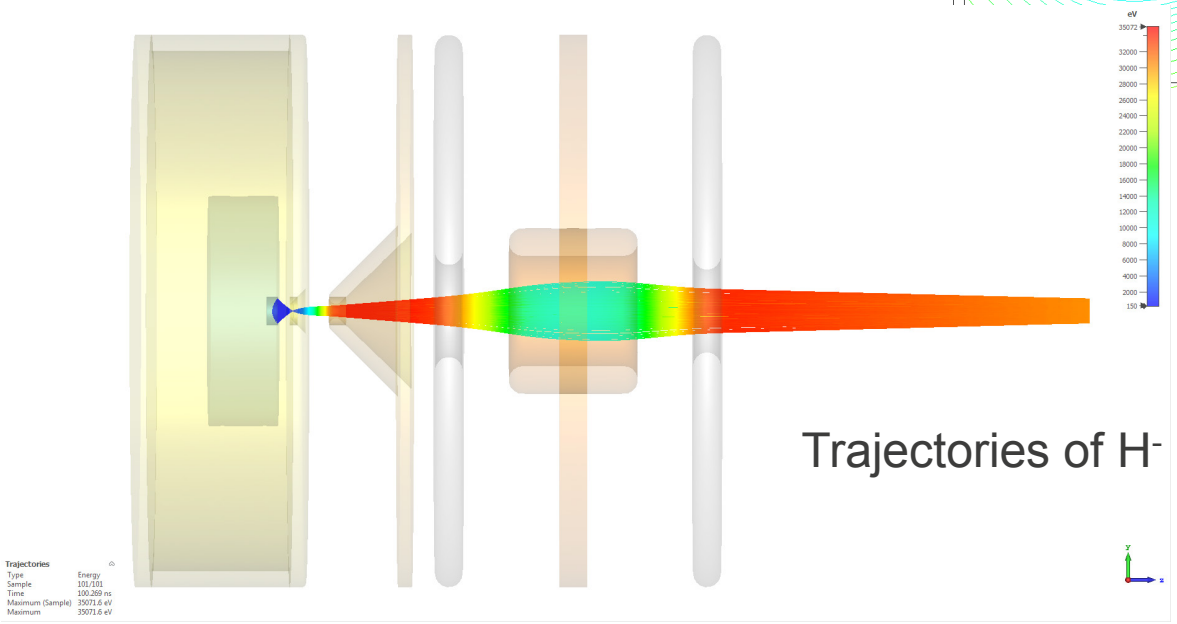

Trajectories of H^- ions

Merging of H^- ion sources

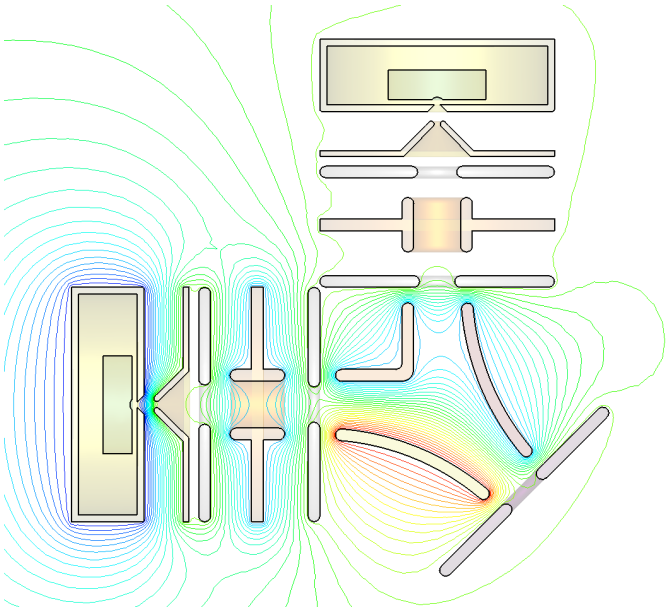

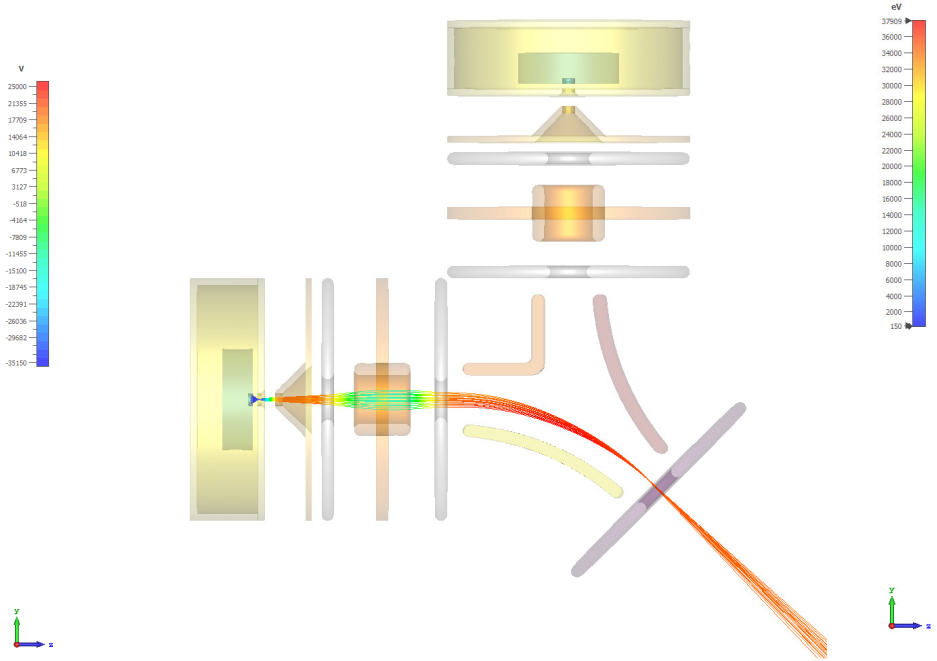

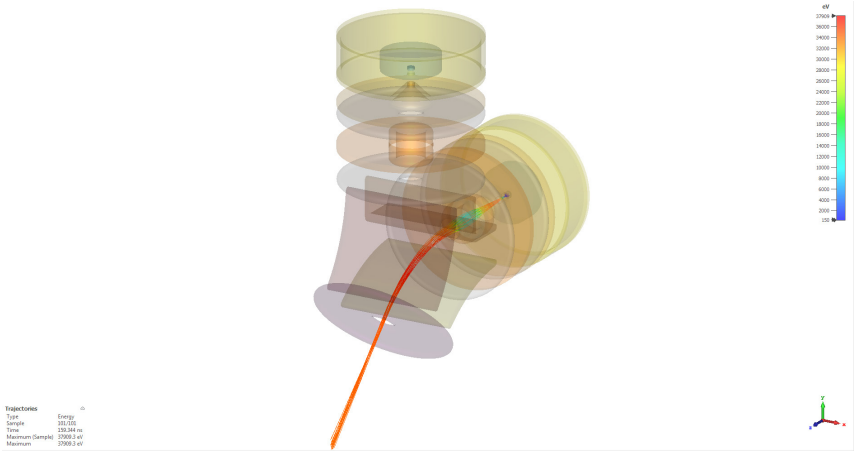

Beam phase space and emittances

Beam emittance is the area occupied by the beam in the phase space. We usually deal with emittance projections, e.g. in (x, $x'=dx/dz$) plane; units mm·mrad. The beam phase space is 6-D; it is 6-D volume that is conserved. The projections can change; emittance exchangers!

Element of phase space: $dV = dx\, dy\, dz\, dP_x\, dP_y\, dP_z$

Phase space density (beam distribution function):

$$f(x, y, z, P_x, P_y, P_z) = \frac{dN}{dx\, dy\, dz\, dP_x\, dP_y\, dP_z}$$

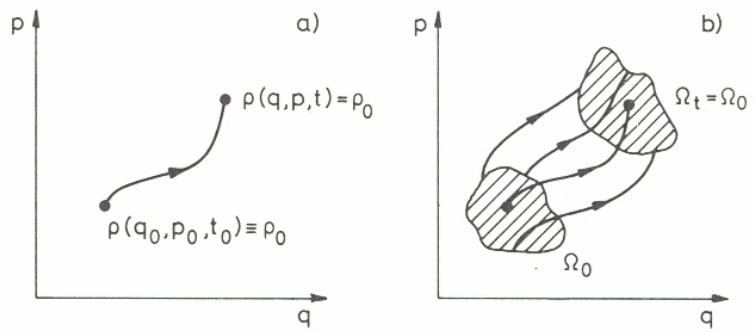

Liouville theorem. If the motion of a system of mechanical particles obeys Hamilton's equations, then phase space density remains constant along phase space trajectories and phase space volume occupied by the particles is invariant.

Liouvillian processes: dynamics in EM fields without dissipation or scattering.

Non-Liouvillian processes: those with dissipation or scattering (e.g. on foil or residual gas, and Coulomb particle-particle interaction), synchrotron radiation.

Liouville's theorem does not allow inserting particles in phase space already occupied by the beam: there are no forces for that. But there are tricks to get around…

Beam cooling: stochastic cooling (CERN, 1980s), electron cooling for protons or ions (e.g., FNAL), and ionization cooling (e.g., for muons) – are non-Liouvillian processes.

Beam phase space – tricks

Example – Charge-Exchange Injection: Two oppositely charged beams can be made to travel along the same trajectory. In the straight section, the beams are passed through a thin foil, which strips the electrons from the H^- ions, leaving a single proton beam of higher density in phase space.

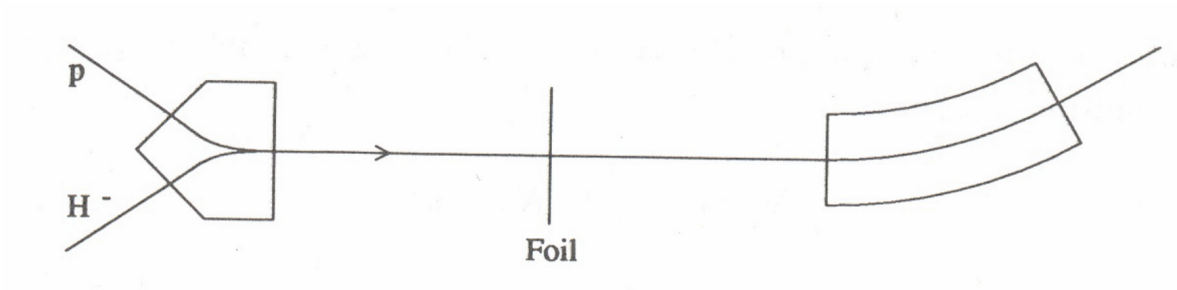

This process is also used for beam accumulation in spallation neutron sources. Multiple pulses from H^- linac are accumulated in a storage ring to be extracted in one short pulse.

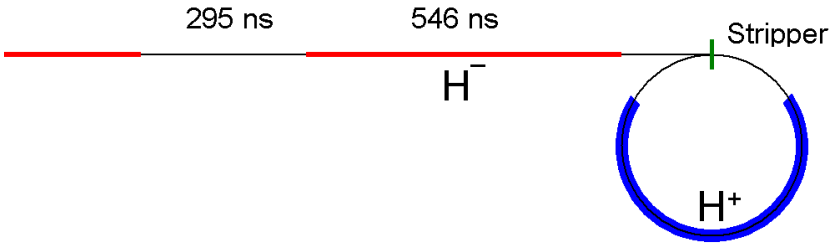

Linac beam accumulation in a ring. The beam gap is for extraction. SNS beam parameters (1998).

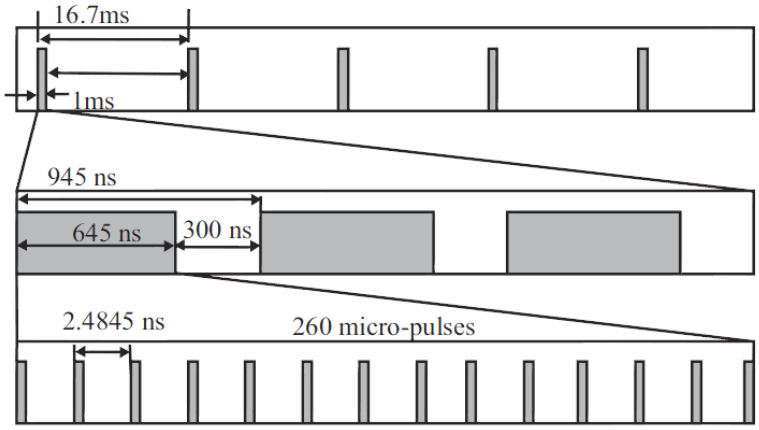

SNS beam pulse structure (now).

Traveling-wave beam choppers

Beam choppers are structures that deflect the beam to a beam stop to create a required pulse pattern. TW choppers – slow-wave structures with $\beta = \beta_{beam}$.

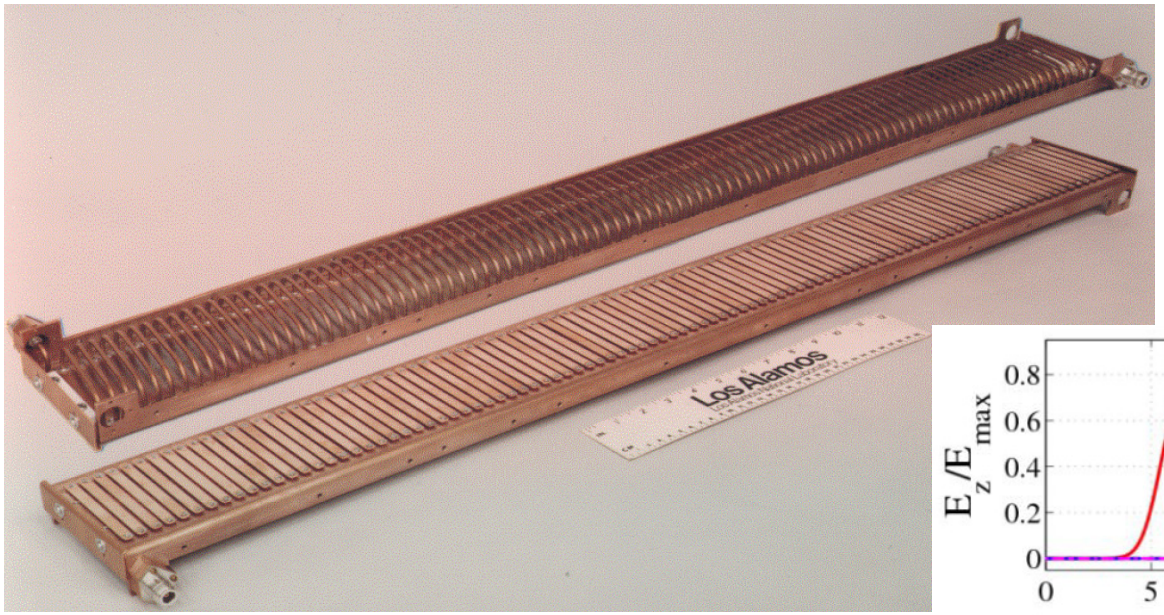

LANSCE strip-coax chopper (1980s)
$\beta = 0.04$
$t_{str} = 2$ ns; $t_{tot} \sim 7$-10 ns

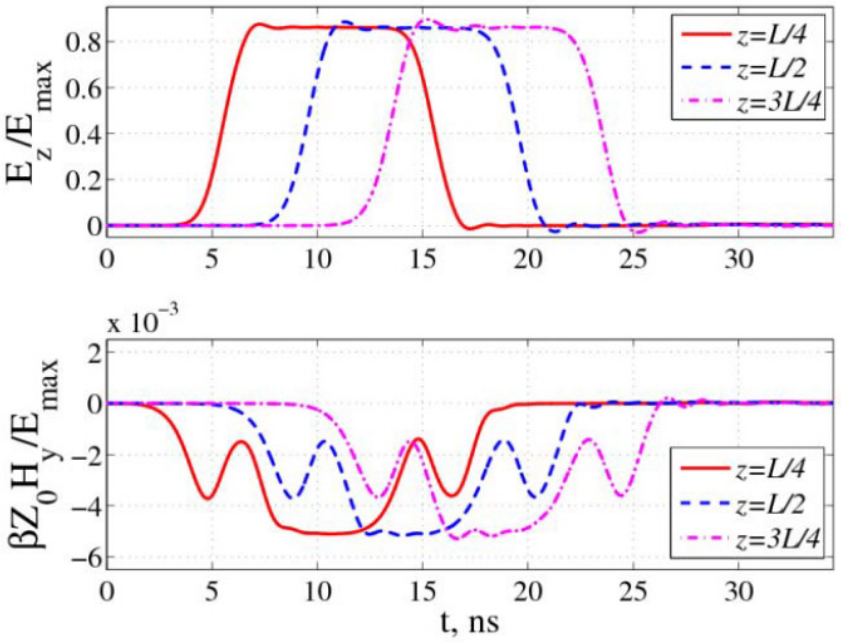

Traveling-wave beam choppers - 2

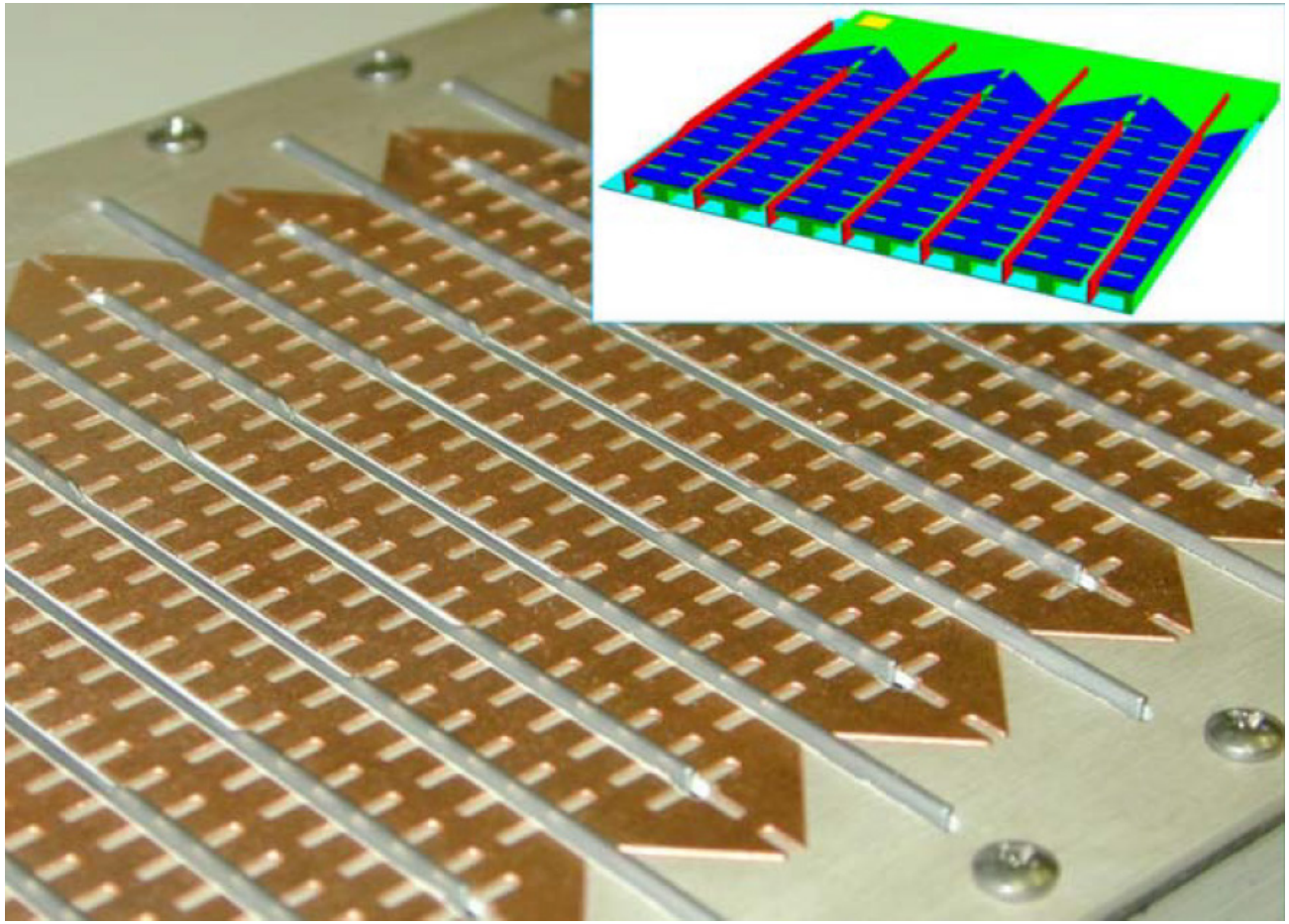

SNS meander-line chopper
$\beta = 0.073$
t_{str} = 1 ns
t_{tot} ~ 2.5 ns
(1999-2007)

Traveling-wave beam choppers - 3

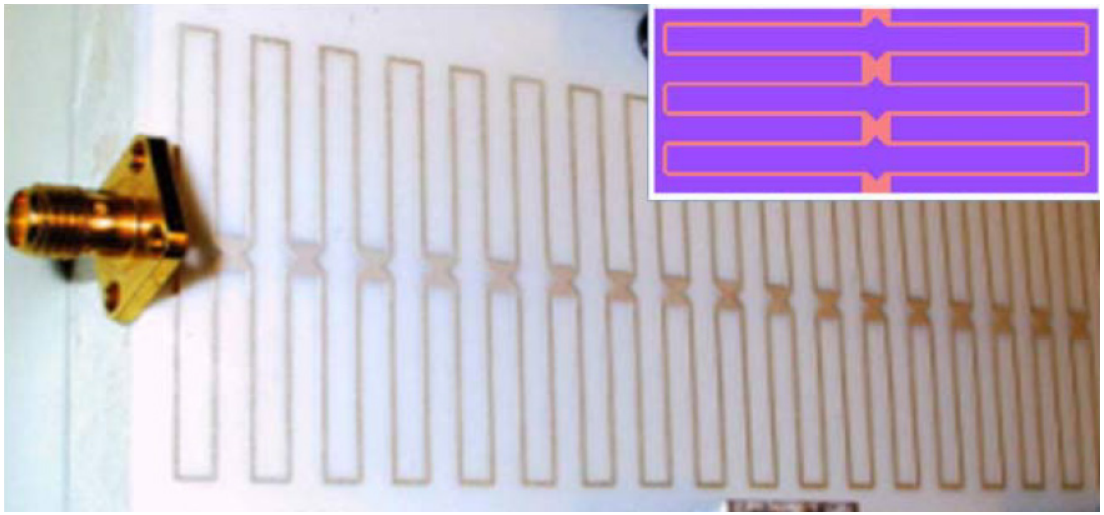

CERN double-meander chopper
β = 0.08
t_{str} = 2.5 ns
(2002)

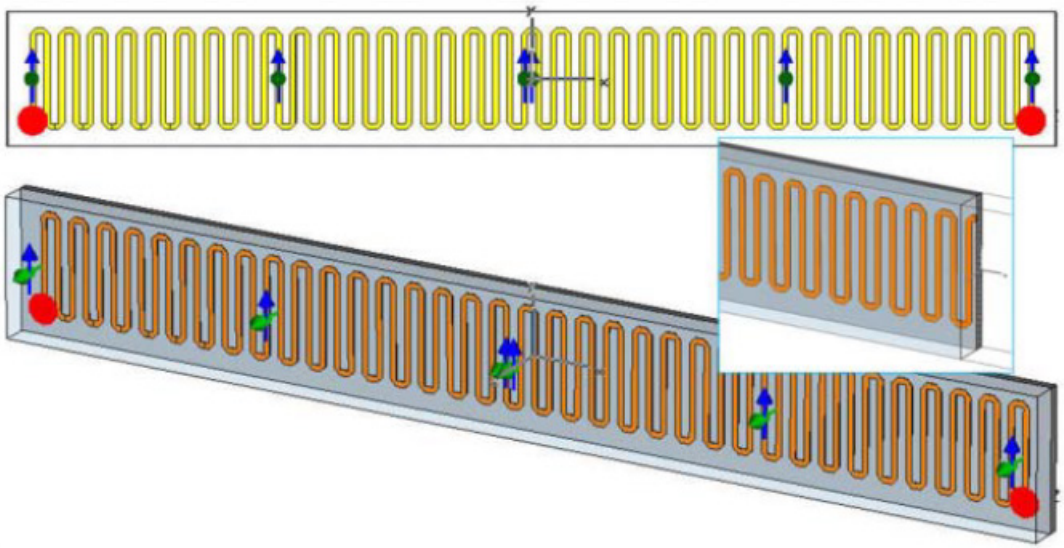

SNS alt. chopper
β = 0.073
t_{str} = 2 ns
(suggested 2007)

Beam emittance

Un-normalized (energy-dependent) and normalized transverse emittance projections:

$$x' = \frac{dx}{dz} = \frac{P_x}{P_z}$$

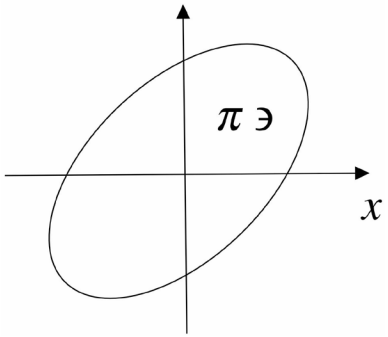

$$\varepsilon_{x,un,rms} = \left(\left\langle (x-\bar{x})^2 (x'-\bar{x}')^2 \right\rangle - \left\langle \left[(x-\bar{x})(x'-\bar{x}') \right]^2 \right\rangle \right)^{1/2}$$

$$\varepsilon_x \equiv \varepsilon_{x,norm,rms} = \beta\gamma\varepsilon_{x,un,rms}$$

Normalized emittance is energy-independent

The ellipse area is $\pi\varepsilon$; units are π m·rad.
Typical transverse emittance values in proton linacs < 1 π mm·mrad.
Meaning $\varepsilon_x \sim \Delta x \cdot \Delta p_x$, $\varepsilon_y \sim \Delta x \cdot \Delta p_y$.

$$\frac{P_x}{mc} = \beta_x\gamma$$

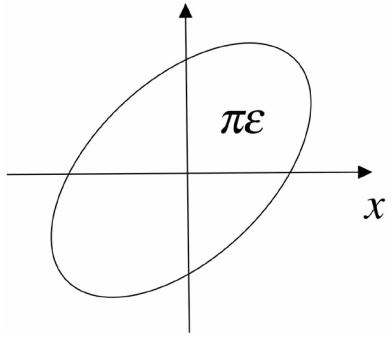

Similarly, the longitudinal emittance $\varepsilon_z \sim \Delta x \cdot \Delta p_z$, can be expressed in the same units, but sometimes $\varepsilon_z \sim \Delta\varphi \cdot \Delta W$ is more convenient. The corresponding units then are MeV·deg.

Summary of part 1

- Linacs and RF are closely related.
- In ion linacs the synchronism between the accelerated particles and RF is achieved by designing the spatial structure with $L_c \sim \beta\lambda$. Fixed velocity profile! Independent-cavity structures can also used, e.g. in heavy-ion linacs, for more flexibility.
- Longitudinal and transverse beam focusing cannot be achieved simultaneously in RF fields. External transverse beam focusing is usually added.
- Basics of beam focusing and phase space are also reviewed.